Ocean Engineering 121 (2016) 323–340

Contents lists available at ScienceDirect

Ocean Engineering

journal homepage: www.elsevier.com/locate/oceaneng

Sensitivity analysis on seismic life-cycle cost of a fixed-steel offshore platform structure

Mohamed Nour Eldin, Jinkoo Kim *

Dept. Civil and Architectural Eng., Sungkyunkwan University, Suwon, Republic of Korea

ARTICLE INFO

Article history:
Received 22 October 2015
Received in revised form
16 February 2016
Accepted 30 May 2016

Keywords:
Life cycle cost
Sensitivity analysis
Seismic design
Offshore jacket platform

ABSTRACT

In this study sensitivity analyses were conducted to investigate the relative importance of different uncertain variables on the life-cycle cost (LCC) estimation of a steel jacket offshore platform subjected to seismic loads. The sensitivity analysis was conducted using different methods such as tornado diagram analysis (TDA), first-order second-moment (FOSM) and Latin hypercube sampling (LHS). The analysis results showed that the uncertain variables related to loss estimation and seismic hazard had a more dominant influence on the LCC variability compared to the other variables. Among the structural uncertain parameters, the variability in plastic hinge strength and modal damping ratio had the most significant impact on the LCC. Variability in the initial cost showed higher impact on LCC estimations compared to other cost component variables. It was also observed that the application of members with energy dissipation capability resulted in more economical design compared to use of conventional members.

1. Introduction

Life-cycle cost (LCC) evaluation of a structure is generally carried out to determine a rational design, retrofit, or maintenance scheme among many possible options. For accurate life cycle cost (LCC) estimation of structures, the uncertainties associated with design variables need to be investigated properly. The more knowledge we have regarding these uncertain variables and their variations, the more reliable and accurate LCC estimations can be obtained. Sensitivity analysis is a useful tool for highlighting the relative impact of input variables on corresponding output response. Life-cycle cost-benefit assessment of seismic risk mitigation activities requires accurate estimation of LCC. These activities provide important source of decision-making supporting information (Goda et al., 2010; Takahashi et al., 2005; Goda and Hong, 2006; Hanai et al., 2003). In addition, accurate LCC assessment plays an important role in performance-based and consequence-based earthquake engineering (Ellingwood and Wen, 2005).

Most of LCC studies have focused on incorporating LCC as an objective function for achieving optimum designs of structures (e.g. Liu et al., 2005; Zou et al., 2007; Wen and Kang, 2001a, 2001b). Other studies are dedicated to using LCC in seismic assessment (e.g. Lagaros, 2007; Gencturk, 2013; Lamprou et al., 2013). However, less attention has been paid to the sensitivity of LCC for different input parameters. Moreover, most of the seismic LCC studies found in literature have focused on conventional structural systems designed using force-based seismic design (e.g. Liu et al., 2004; Ang and Lee, 2001; Beck et al., 2003). In addition, most of current studies give less concern to the impact of soil-pile-structure interaction (SPSI). However, consideration of SPSI significantly affects the seismic fragility of pile-founded structure (Kwon and Elnashai, 2010) which has a direct effect on the LCC estimation.

Sensitivity analysis is generally performed to identify the relative importance of design variables. Padgett and DesRoches (2007) studied the sensitivity of a multi-span simply supported steel girder bridge. Kim et al. (2011) studied the sensitivity of design parameters of steel buildings subjected to progressive collapse. Celarec et al. (2012) investigated the sensitivity of seismic response parameters to the uncertain modeling variables of four infilled RC frames using pushover analysis. Zona et al. (2012) conducted a response sensitivity analysis to study the effects of brace over-strength distributions of steel frames with buckling-restrained braces (BRBs) on the expected maximum reduction of seismic performance as measured by local and global engineering demand parameters (EDPs). Recently, Nour El-Din and Kim (2014) conducted a sensitivity analysis of pile-founded fixed steel jacket platforms subjected to seismic loads.

They also conducted seismic performance evaluation of jacket platforms with various bracing types (NourEldin and Kim, 2015).

In the current study, a steel jacket offshore platform in Gulf of

* Corresponding author.
E-mail address: jkim12@skku.edu (J. Kim).

http://dx.doi.org/10.1016/j.oceaneng.2016.05.050
0029-8018/

Notations

a and b	are the regression coefficients for linear regression of drift demand D on intensity S_a in logarithmic space
k_o and k	are the coefficients for linear regression of hazard $H(s_a)$ on intensity S_a in proximity of limit state probability (region of interest) in logarithmic space.
C_i	corresponding cost of exceeding a specific limit state
C_o	initial construction cost which will be related to the material cost in the current study
$\hat{D}$	median drift demand
D_1	damage index of the platform, which can be expressed as the ratio between the actual and allowable maximum inter story drift ratios.
D_R	repairable damage index
EDP_j	LCC estimated at the jth simulation
$K_{i,j}$	prescribed correlation coefficients between the random variables X_i and X_j
N_{Sim}	number of simulations
N_{Var}	number of random variables
P_{LS}	annual probability of exceeding a specific limit state
Q_d	pile ultimate bearing capacity
Q_f	pile skin friction resistance
Q_p	pile total end bearing
R_C	replacement cost
S_a^C	spectral acceleration corresponding to the median drift capacity
S_a	elastic spectral acceleration (measure of ground motion intensity)
S_a	spectral acceleration (measure of ground motion intensity);
$S_{i,j}$	generated correlation coefficients between the random variables X_i and X_j
$x_{j,i}$	value of the i^{th} input random variable for the jth simulation
β_C,	drift capacity dispersion measure
$\beta_{D\mid S_a}$	drift demand dispersion measure
ρ_i	Spearman rank-order correlation coefficient
[R]	Matrix of ranking coefficients
[S1]	matrix of correlation
BRB	buckling restrained brace
C_m	maintenance cost
COV	coefficient of variation
CP	collapse prevention limit state
E	norm measuring the difference between the generated and the prescribed correlation matrices
$E[C_{SD}]$	annual expected seismic damage cost
EDP	engineering demand parameter
FB-BRB	steel jacket structural model of the platform that designed using buckling-restrained bracing
FB-Conv	steel jacket structural model of the platform designed using the conventional bracing
FOSM	first-order second-moment
F_y	specified minimum yield strength of steel
$H(s_a)$	hazard function of spectral acceleration, annual probability that intensity S_a at site will equal or exceed s_a
IO	immediate occupancy limit state
L	service life of the structure
LCC	life-cycle cost
LHS	Latin hypercube sampling
LS	life safety limit state
MCE	maximum considered earthquake
N	total number of limit-states considered,
N_{Sim}	number of simulation
p	lateral soil reaction (p) per unit length of the pile
PGA	peak ground acceleration
p_i	total probability that the structure is in the ith damage state throughout its lifetime,
P_u	required axial strength
P_{ysc}	design strength of a steel cross section.
R	rank of the jth sample value of the input random variable
R	response modification factor according to ASCE-7 (2010)
R_y	over strength factor
S_{D1}	design, five percent damped, spectral response acceleration parameter at a period of 1 second
S_{DS}	design, five percent damped, spectral response acceleration parameter at short periods
SPSI	soil-pile-structure interaction
TDA	tornado diagram analysis
X	the sample matrix of the random variables, where the number of rows and columns are representing the number of simulations and number of input variables, respectively
$X_{bearing}$	random variable of pile end bearing
X_{cyclic}	random variable of cyclic nature of the loading
X_{delay}	random variable of set-up or effect of time since the pile is driven or last disturbed
$X_{friction}$	random variable of shaft friction between soil and pile
y	lateral pile displacement
α	discount factor which is equal
β	compression adjustment factor
$\Delta_{C,i}$	is the structural capacity, represented in terms of drift ratio, defining the ith damage state
Δ_D	earthquake demand, represented in terms of drift ratio
ϕ	strength reduction factor
λ	annual discount rate, and
ω	strain hardening adjustment factor

Moattam, offshore of Myanmar, designed considering soil-pile structure interaction, is used as a case study. Different bracing types, such as buckling-restraint braces and conventional braces, are applied in the platform design to investigate their effect on the seismic LCC of the platform structures. Sensitivity analysis is performed using tornado diagram analysis (TDA), first-order second-moment (FOSM), and Latin hypercube sampling (LHS) techniques. The effects of both aleatory and epistemic uncertainty on LCC have been investigated for this platform. The sources of uncertainty considered in the present sensitivity study are categorized into different categories: (1) the structure capacity and modeling, e.g. related to stiffness or damping characteristics, etc.; (2) the SPSI modeling, e.g. soil-pile friction capacity, pile end-bearing capacity, etc.; (3) the seismic hazard, e.g. the probability of occurrence; (4) the loss-estimation socioeconomic criteria and cost components, e.g. damage limit states, initial cost, limit state exceedance cost, annual discount rate, etc.

2. Sensitivity analysis methods applied

In order to have enough confidence in any sensitivity analysis results, it is important to monitor the variation of the input parameters and the corresponding output response quantity with different methods. In the present study, three different methods have been adopted in the sensitivity analysis of the offshore platform structure under investigation. These methods are based on the probability theory, which are the Tornado Diagram Analysis (TDA), the First-Order Second Moment (FOSM), and the Latin Hypercube Sampling (LHS) methods. The methods used in the current study proved, in previous studies, to have simplicity in implementation while maintaining the required efficiency. In general, these methods are useful tools for sensitivity studies where Monte Carlo Simulation (MCS) is not affordable.

In Tornado Diagram Analysis (TDA), which is a common tool for decision analysis (Porter et al., 2002), the upper and lower bounds of a random variable are used to obtain the variability in the output value. Through any LCC model, the difference between such estimations, referred to as swing, is considered as a measure of the seismic LCC sensitivity. This method has been applied in the seismic sensitivity analysis of structures in many previous studies (e.g., Porter et al., 2002; Barbato et al., 2010; Kim et al., 2011). This method makes a direct relation between the uncertain input variable and the output value of the EDP through a deterministic function. A few simulations are generally sufficient to determine the required variability in the selected EDP. The limitation of this method is that the output is determined through a known deterministic function of a variety of input variables, and that either the value or the probability distribution of each of the input variables is specified (Porter et al., 2002). If the function is not deterministic, this method will not be useful and another probabilistic approach should be used.

In First-Order Second Moment (FOSM) method, the mean and standard deviation of the input parameter are predetermined and the mean and standard deviation of the structural response are obtained. The FOSM method is formulated in a Gaussian space, and involves a small number of structural analyses in comparison with some other methods such as Monte Carlo simulation. The method has been used in many previous studies (e.g. Ibarra, 2003; Haselton, 2006; Baker and Cornell, 2003, 2008; Celarec and Dolšek, 2013). The details of the method can be found elsewhere (e.g. Lee and Mosalam, 2005). Assuming that the LCC model is a deterministic function, the variation in any input parameter will result in variation of the LCC estimation.

The limitation of this method is that, in the nonlinear functions, the mean and variance may be very difficult (or even impossible) to derive analytically. In this case, MCS would be necessary (Ang and Tang, 2007).

Latin Hypercube Sampling (LHS) method uses stratification of the probability-distribution function of the random variables and consequently requires significantly fewer simulations in comparison with Monte Carlo simulation method. The details of the method can be found elsewhere (e.g. Vorechovsky and Novak, 2003; Dolsek, 2009; Celarec and Dolšek, 2013). In the current study, the number of simulation (N_{Sim}) is assumed twice the number of the input variables (N_{Var}). This assumption has been recommended in previous studies (e.g. Celarec and Dolšek, 2013; Dolsek, 2009) to maintain the required effectiveness of the sample and to achieve a sufficient accuracy of the results. In this case, the norm E, which is an indicator to the sample effectiveness, is maintained as minimum. The norm E is a measure of the difference between the generated and the prescribed correlation matrix, which is given as,

$$E=\frac{2}{N_{Var}\left(N_{Var}-1\right)}\sqrt{\sum_{i=1}^{N_{Var}-1}\sum_{j=i+1}^{N_{Var}}\left(S_{i,j}-K_{i,j}\right)^2} \tag{1}$$

where $S_{i,j}$ and $K_{i,j}$ are, respectively, the generated and the prescribed correlation coefficients between the random variables X_i and X_j, and N_{Var} is the number of random variables. In the current study, Matlab programming language (Mathwork, 2011) is used for achieving minimum norm E through Simulating Annealing technique. $S_{i,j}$ and $K_{i,j}$ are related to the norm E (an objective function), which should be minimized. This minimization is achieved through two steps: mutation and selection. Mutation represents the random change of the rank of one randomly selected random variable. This can be achieved by exchanging rank m to become rank n and vice versa in a vector (column) from the sample matrix **X**, which represents the sample of one random variable. After such a mutation, the sample matrix **X** is changed and the new norm E can be calculated. The second step, selection, decides if the new generation of the arrangement of the sample matrix **X** is acceptable or not. Further details about this technique can be found in Vorechovsky and Novak (2003). The Spearman rank-order correlation coefficient (ρ_i) is used to measure the sensitivity of the LCC to the input random variables (Vorechovsky and Novak, 2003; Kala, 2005). For the i^{th} input random variable, the (ρ_i) coefficient is expressed as

$$\rho_i=1-\frac{6\sum_{j=1}^{N_{Sim}}\left(r\left(x_{j,i}\right)-r\left(\mathrm{EDP}_j\right)\right)^2}{N_{Sim}\left(N_{Sim}^2-1\right)} \tag{2}$$

where $x_{j,i}$ is the value of the random variable for the jth simulation, taken from the optimized sample matrix, EDP_j is the LCC estimated at the jth simulation, N_{Sim} is the number of simulations, and r denotes the rank of the jth sample value of the input random variable or response variable. The range of ρ_i is $-1.0 \le \rho_i \le 1.0$; the closer the ρ_i coefficient goes to zero, the less dependent the output response becomes on this variable.

The limitations of the LHS method can be summarized as: 1) this method gives relative importance of the input uncertain variable. No swing value can be obtained using LHS as in the case of FOSM or TDA methods; 2) this method is sensitive to the assumed number of simulations. Special care should be given to the number of simulation especially for small number of input variables; 3) in case large number of variables are involved, the number of simulation will be large. In this case, LHS method may be computationally expensive option.

As shown from the above discussion regarding the sensitivity methods, the approach for each method is different to examine the impact of the input variable on the required EDP. In TAD and FOSM methods, the mean and standard deviation of the input parameter are predetermined, and based on that the mean and standard deviation of the structural response are obtained. However, in LHS method, simulations are conducted to arrange the variables based on their relative importance when the ranges of the input variables are stratified. This adds more reliability in the results as the relative importance of the input variables are checked through different approaches.

3. Design and modelling of jacket

3.1. Jacket structure

The platform has the topside with four-stories and a four-story jacket with total mass of 138,000 ton located in the main nodes of the jacket. Only the major structural components are included within the analysis model, and the contribution of the conductors to the platforms' stiffness and strength is neglected. A perspective plot of the platform is shown in Fig. 1(a), a plan view of the jacket is shown in Fig. 1(b), and a 2D-frame model extracted from the platform structure is shown in Fig. 1(c). In this study, all analyses are conducted on the representative 2D-frame models. The brace elements are modeled as truss elements and Jacket legs are modeled

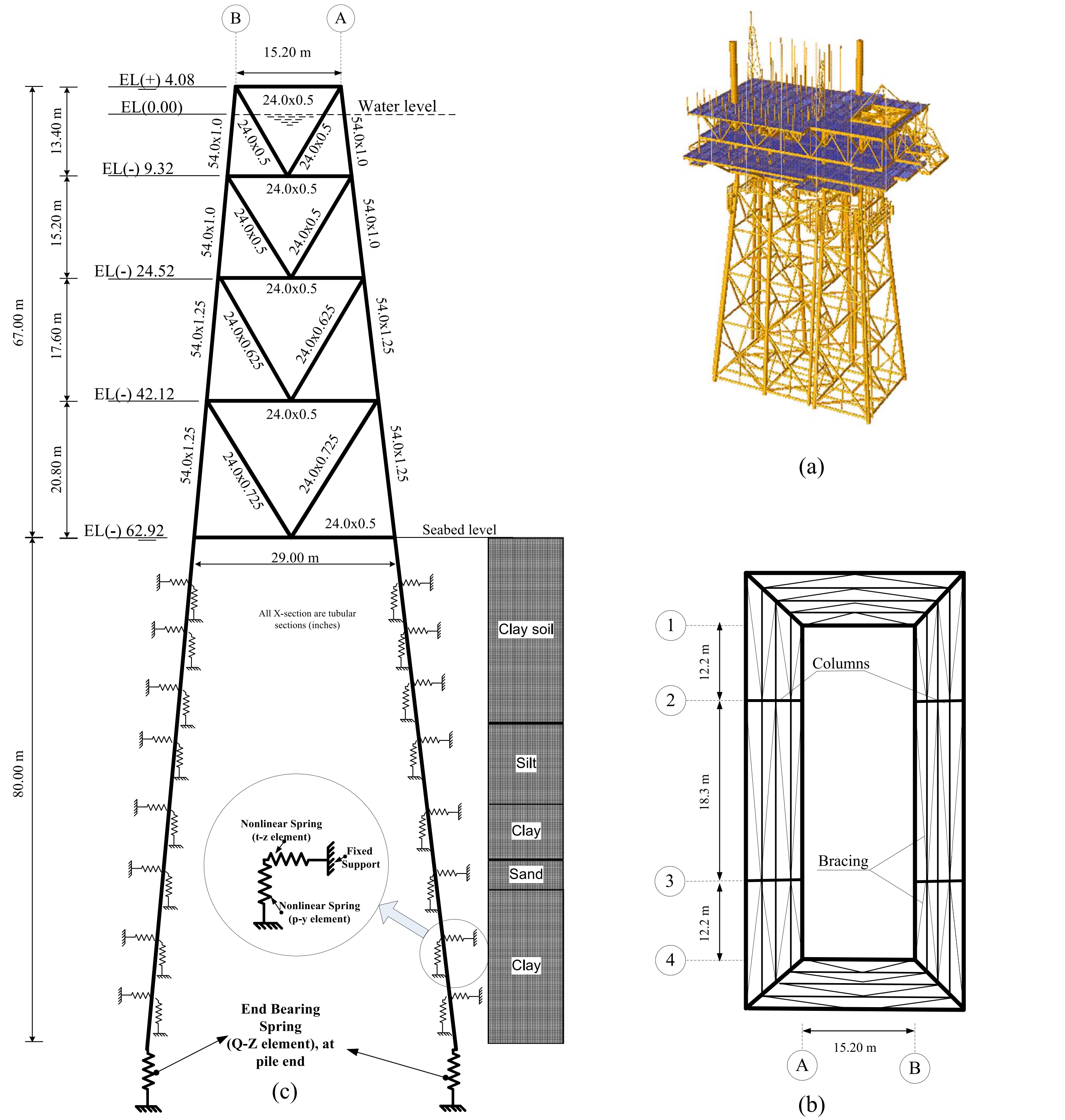

Fig. 1. Jacket structure schematic views, (a) perspective plot of the actual platform; (b) plan view of the jacket; and (c) 2-D single frame extracted from the actual platform with the soil-pile configuration.

as frame elements (beam-columns). The jacket horizontal members are frame elements (beams) pin-connected at the ends. A pinned beam-column-brace connection is used at all story levels to avoid undesirable connection failures due to unbalanced brace forces. The model structures are designed with compact sections so that local buckling is prevented. The local behaviors of joints are not considered based on the assumption that they are designed to be stronger than elements using larger safety factor.

The mass used in the dynamic analysis consists of the mass of the platform associated with gravity loading defined, the mass of the fluids enclosed in the structure and the appurtenances, and the added mass. The mass of the model frame is applied at each joint, while the mass from the top side structure is applied at the upper two joints of the jacket frame. The nonlinear dynamic analyses of the model frame structure are carried out using the SAP2000 Software (2005). A frame element with plastic hinges is chosen from the SAP2000 library to model the nonlinear behavior of platform members. The modal damping ratio of 5% of critical damping is generally used in the analysis of offshore structures (API RP-2A, 2000), which includes the effect of water-structure interaction and the foundation and structure related energy dissipation effects.

In order to investigate the effect of the ductility on the LCC sensitivity to the input variables, the platform is designed using two different bracing systems: the conventional bracing (FB-Conv) and the buckling-restrained bracing (FB-BRB). The former is designed using R (response modification factor)=3.25, and the latter is designed using R=7.0 according to ASCE-7 (2013). Detailed information of the analysis model structures and design parameters can be found in Nour El-Din and Kim (2014).

The design base shears of the force-based designed model structures are obtained in accordance with ASCE-7 (2013). The seismic design base shear is computed using the site-specific response spectrum, which corresponds to 2/3 of the maximum considered earthquake (MCE) with 2% probability of occurrence in 50 years in the Gulf of Moattama, offshore of Myanmar. For force-based design of the structures in accordance with the ASCE-7, the nominal yield strength of materials used for all elements is 380 MPa with the material over strength factor, R_y, of 1.1. A buckling restrained brace (BRB) has a core element enclosed in a buckling-restrainer and therefore yields in both tension and compression. The steel core areas of BRBs are calculated using the following relation suggested in the AISC341-05: $P_u < \phi P_{ysc}$, where P_u is the required axial strength and ϕ is the strength reduction factor of 0.9 for both tension and compression, $P_{ysc}$is the design strength which is equal to $F_y A_{sc}$, where F_y and A_{sc} are the specified minimum yield strength and net area of steel core, respectively. In the FB-BRB model, the demand on beams and columns is obtained based on the expected yield and ultimate strengths of BRBs in tension and compression by applying material overstrength factor, R_y, compression adjustment factor, β, and the strain hardening adjustment factor, ω. The values of these factors are shown in Table 1. In the case of conventional braces, the demands on beams and columns are obtained based on the expected tensile yield and buckling strength of braces.

3.2. Soil-pile-structure interaction (SPSI)

In the present study, the Beam on Non-Linear Winkler Foundation (BNWF) model is applied to approximate the interaction between the pile and the surrounding soil (Matlock, 1970), in which parallel nonlinear soil-pile springs are used along the pile penetration length. This model simplifies the interaction between the soil and the pile by assuming that the displacement of one spring has no effect on the displacement of other springs. The lateral soil stiffness is modeled using the p–y approach. In this approach, for each layer of soil along the depth, a nonlinear relationship is established between the lateral pile displacement (y) which mobilizes the lateral soil reaction (p) per unit length. The procedure of generating p–y curves is recommended in American Petroleum Institute Standard API RP-2A (2000). In the present study, p-y curves are based on the actual soil data extracted from the geotechnical report of the platform site (PTTEP International, 2010). In the numerical model proposed in this paper, the Multi-Linear Plastic type link element in SAP2000 is used to model the non-linear lateral relation between the soil and the pile. In that link element, the nonlinear link stiffness for the axial degree of freedom is defined according to the p-y curve. Then the p-y curve is redefined as a force-deformation (*F-D*) relationship where *F* is the total force acting along the tributary length of a pile joint. After that, a lateral link is defined for each joint along each unit pile segment to represent the lateral soil non-linear behavior. Fig. 2 shows the configuration of the proposed model in SAP2000. A multi-linear kinematic plasticity property type is selected for uniaxial deformation from the SAP2000 library to model the hysteresis of the non-gapping soil behavior.

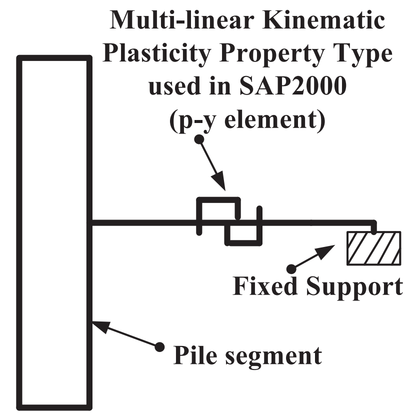

Fig. 2. Configuration of lateral soil stiffness modeled in SAP2000.

The skin friction and the end bearing between a pile and the surrounding soil produce the soil resistance to the axial movement of the pile. Each of the resistance action is characterized by a nonlinear force-deformation relationship. Experimental results suggest that these force-deformation characteristics may be adequately represented by the elastic, perfectly-plastic relationship (Anagnostopoulos, 1983, Coyle and Reece, 1966) as shown in Fig. 3.

Frame element is chosen from the library of the SAP2000 to model the behavior of a pile. The diameter of the pile is 1,210 mm and penetrates into 80 m in the soil. In order to simulate the structure-pile–soil interaction through several layers of different soils, the piles are divided along their vertical axis such that within each layer of the soils the portion of the pile is divided into 1.0 m long segments. The relative movement between the pile and soil can be simplified into a number of non-linear vertical springs representing the vertical friction force exerted by the soil on the pile surface. For each pile, there is also an end support spring, which represents the end-bearing capacity of the pile. Fig. 4 illustrates the arrangement of the vertical and end bearing soil springs. The spring parameters are calculated according to the site investigation and pile testing data (PTTEP International, 2010).

Table 1
Design parameters for model structures.
(a) FB-BRB and (b) FB-Conv models.

S_{DS} (g) S_{D1} (g)	1.0 0.7
Framing type	BRBF (FB-BRB) OCBF (FB-Conv)
Response Modification Factor, R	7 (FB-BRB) 3.25 (FB-Conv)
Importance factor, I	1
Occupancy category	II
Seismic design category	D
Base shear coefficient (base shear/structure weight)	0.052 (FB-BRB) Base shear = 1941 kN 0.11 (FB-Conv) Base shear = 4107 kN
Fundamental period (s)	2.75 (FB-BRB) 1.8 (FB-Conv)

4. Uncertain variables considered in the analysis

In this section, the uncertain parameters considered in the sensitivity study are discussed and the associated ranges or probabilistic distributions are addressed for each input variable.

4.1. Structure capacity and modeling uncertainty

The statistical properties of structural modeling parameters are listed in Table 2. All variables are assumed uncorrelated. In the current study, the variation of plastic hinge property is obtained by

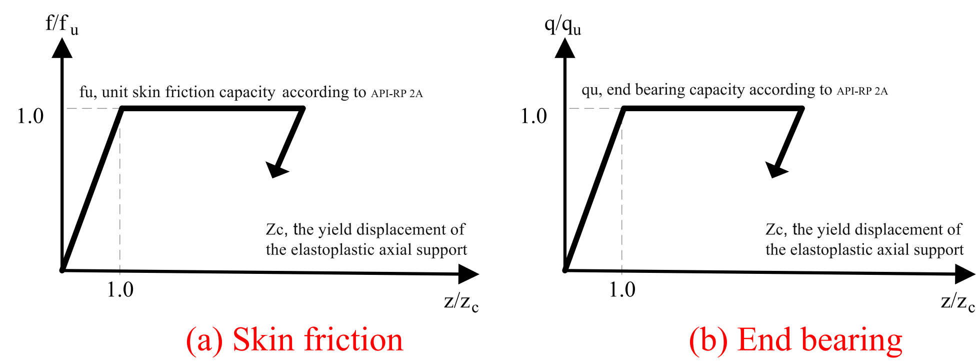

Fig. 3. Axial load-deflection curves for clays and sands (Anagnostopoulos, 1983; Coyle and Reece, 1966). (a) Skin friction. (b) End bearing.

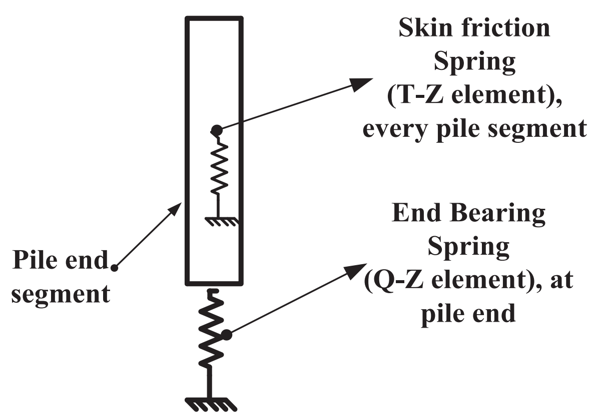

Fig. 4. Schematic illustration of the pile spring model.

scaling every force and deformation value on the force-deformation relationship by multiplying a single, random variable; this technique is called "random strength-constant stiffness" (Porter et al., 2002).

4.2. Uncertainty of soil-pile structure

Uncertainties associated with soil-pile modeling parameters include the axial pile-soil friction, the pile end bearing, the effect of time since the pile is driven, and the cyclic nature of loading during the pile driving.

The capacity prediction equation for piles in clay soil under compression is as follows (ISO-19902, 2003):

$$Q_d = (Q_f \cdot X_{friction} \cdot X_{delay} + Q_p \cdot X_{bearing}) X_{cyclic} \tag{3}$$

where Q_d is the pile ultimate bearing capacity, Q_f is the pile skin friction resistance; Q_p is the pile total end bearing; and $X_{friction}$, X_{delay}, $X_{bearing}$, and X_{cyclic} are the random variables of the shaft friction, the set-up or effect of time since the pile is driven or last disturbed, the end bearing, and the cyclic nature of the loading, respectively. The statistical properties of these random variables are listed in Table 3.

4.3. Uncertainty of seismic hazard

The hazard function of spectral acceleration, $H(s_a)$, is the annual probability that intensity s_a at site will equal or exceed a specific response acceleration at a given response period s_a. It can be obtained by Eq. (4) as follows:

$$H(s_a) = P[S_a \geq s_a] = k_o s_a^{-k} \tag{4}$$

where s_a is the elastic spectral acceleration (measure of ground motion intensity); $H(s_a)$ is the hazard function of spectral acceleration, annual probability that intensity S_a at site will equal or exceed s_a; k_o and k are the coefficients for linear regression of hazard $H(s_a)$ on intensity S_a in proximity of limit state probability (region of interest) in logarithmic space. These coefficients control the slope and the degree of nonlinearity, respectively, of the hazard curve (Aslani and Miranda, 2005).

In general, the seismic hazard is modeled by a lognormal distribution. The lognormal standard deviations for the earthquake source, transmission path, and local site response are estimated in previous studies as 0.30 (Newmark et al., 1973), 0.70 (Donovan, 1973), and 0.41 (Hays, 1980), respectively (Choun and A.S. Elnashai, 2010). In general, the coefficient of variation (COV) of spectral acceleration is highly dependent on the reliability of the seismic knowledge of the location under investigation. Choun and A.S. Elnashai (2010) used various seismic hazards with five different median PGAs (i.e., 0.1 g; 0.3 g; 0.6 g; 1.0 g, and 1.5 g) and two standard deviations (i.e., .30 and 0.60) to investigate applicable hazard levels of his proposed procedure. Since there is no sufficient information regarding the seismicity of Gulf of Moattama, the COV spectral acceleration will be assumed 0.5in the current study.

The slope of seismic hazard (k) is the power coefficient for

Table 2
Statistical properties of structural modeling parameters.

variable	Distribution	Mean value	Mean bias	Standard deviation	Source of data
Dead load, (Tonf)	Normal	13,800	1.0	0.06	ISO 19902 (2003)
Yield stress, MPa	Lognormal	380	1.1	0.05	ISO 19902 (2003)
Young's modulus, MPa	Normal	200000	1.0	0.05	ISO 19902 (2003)
Damping ratio[a], %	Lognormal	5.0	1.0	0.40	Kim et al. (2011)
Plastic hinge property[b]	Normal	–	1.0	0.20	Ellingwood et al. (1980)

[a] Percentage of critical damping (assumed as steel braced frames). The mean value is assumed as recommended by API-RP2A (2000).
[b] Depends on the plastic properties of the element.

Table 3
Statistical properties of the random variables associated with normally consolidated clay soil.

Variables	Distribution	Mean bias	Standard deviation	Source of data
Soil-Pile Axial Friction, ($X_{friction}$)	Lognormal	0.73	0.19	Smith et al. (1998)
Soil-Pile End Bearing, ($X_{bearing}$)	Lognormal	0.91	0.43	Smith et al. (1998)
Pile Driving Cyclic Load, (X_{cyclic})	Lognormal	1.00	0.07	ISO 19902 (2003)
Pile Driving Time Delay, (X_{delay})	Lognormal	0.86	0.02	ISO 19902 (2003)

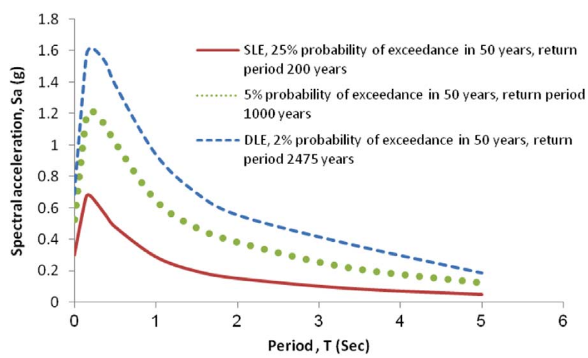

Fig. 5. Design spectra of earthquakes with different return periods obtained at gulf of Mottama, offshore Myanmar. (SLE: strength level earthquake; DLE: ductility level earthquake).

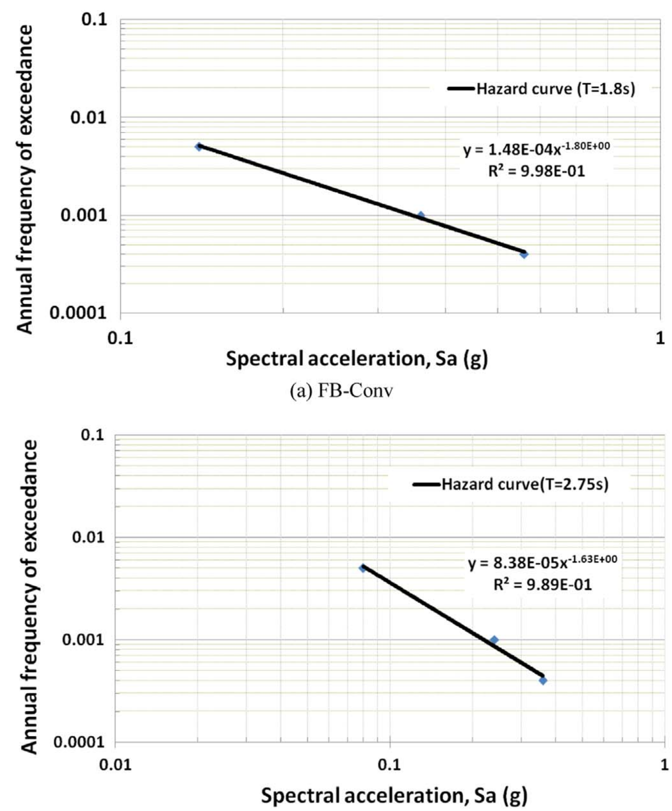

(a) FB-Conv

(b) FB-BRB

Fig. 6. Site seismic hazard curves for the model structures. (a) FB-Conv. (b) FB-BRB.

linear regression of hazard $H(s_a)$ on intensity s_a in proximity of limit state probability in logarithmic scale or, simply, the logarithmic slope of the hazard curve at the desired hazard level. The typical value of this parameter, as suggested in the previous studies (El nash; Cornell et al., 2002; Dolsek, 2012), may be between 1.0 and 4.0. It tends to be larger (steeper) for high seismic areas, e.g. western U.S. sites, and for shorter periods. In the current study, it is found that, for the selected offshore platform models and soil condition, k value ranges between 1.5 and 2.1.The COV of this parameter will be assumed to be in the range of 0.2 to 0.25.

Fig. 5 shows the platform site-specific response spectra of three different return periods of 200, 1000, 2475 years. The seismic hazard curves for different period, T=1.80 s and 2.75 s, are shown in Fig. 6. These periods are the natural period of FB-Conv and FB-BRB models, respectively. Each point on the curve relates the spectral acceleration at the natural period of the model structure (which obtained from the design spectra in Fig. 5) with the corresponding annual frequency of exceedance of each hazard.

4.4. Uncertainty of loss-estimation parameters

The parameters related to loss estimation are the drift-capacity dispersion measure, drift demand dispersion measure, regression coefficient for drift-intensity relation, sensitivity factor, capacity margin ratio, etc. The drift capacity dispersion measure, β_C, is considered to be the structural limit state dispersion. The description of uncertainty in system capacity is complicated since a structural system consists of many components and the system behavior is complex under seismic excitation, especially when the system goes into nonlinear range. The system capacity can be more conveniently described in terms of the system limit states of interest. The uncertainty in capacity against collapse can be described in terms of the mean and standard deviation of the inter-story drift capacity under multiple recorded ground motions from incremental dynamic analysis (IDA). More details about how the global capacity is determined is given in the FEMA 350 and 351 guidelines (2000) and Yun and Foutch (2000). The coefficient of variation of this displacement capacity is in the range of 30% as used in the FEMA/SAC procedure (Wen et al., 2004). In other studies, e.g. HAZUS (2003), epistemic uncertainty in the damage-state threshold of the structural system is given as 0.4 for all the structural damage states and building types. Variability (i.e., aleatory uncertainty) in the capacity properties of the model building type is given as 0.25 for buildings designed by seismic design code and 0.30 for buildings designed by non-seismic design code (Choun and Elnashai, 2010). Based on this information, in the current study, a value of 0.3 for the COV is used.

The drift demand dispersion measure ,$\beta_{D|S_a}$, is a dispersion measure for seismic drift demand at a given spectral acceleration level. Cornell et al. (2002) suggests a value of $\beta_{D|S_a}$ in the range of 0.3 or more based on Luco and Cornell (2000) and Yun and Foutch (2000). Previous works of Lagaros et al. (2005, 2007) suggest that the coefficient of variation of the maximum inter-story drift of an RC structure is close to 10% when uncertainties in both material properties and seismic excitation are taken into account. In the current study, the dispersion in earthquake demand ($\beta_{D|S_a}$) due to variability in groundmotions is established using two sets of earthquake ground motions each representing a different hazard level at return periods of 200 and 2475 years. The details of the records are given elsewhere (Nour El-Din and Kim, 2014). For the current study, COV in $\beta_{D|S_a}$ is taken as 0.3. It is worth mentioning that $\beta_{D|S_a}$ is assumed to be the same for the different seismic

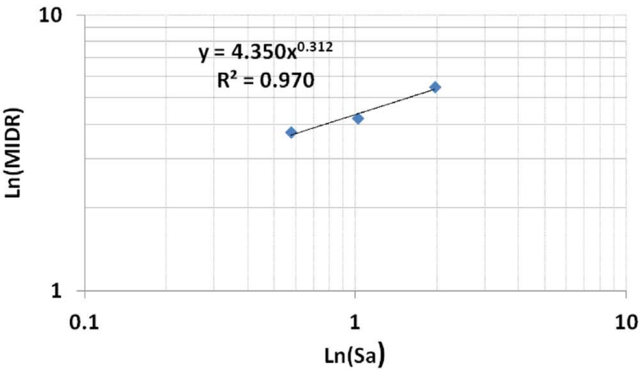

(a) FB-Conv

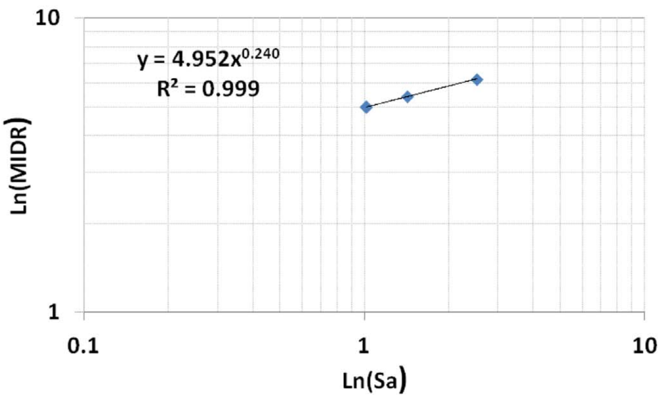

(b) FB-BRB

Fig. 7. Relation between median inter-story drift demand *(MIDR)* and seismic intensity (S_a). (a) FB-Conv. (b) FB-BRB.

hazard. This is because of using a scaling method that minimizes the dispersion in demand. In this method of scaling, the ground motion records obtained from PEER database (PEER, 2013) are scaled in such a way that the geometric mean of the response spectra for the records matches the uniform hazard spectrum over a period range corresponding to the fundamental period of the structure. In addition, this scaling method takes into account the elongation of the structural period due to non-linear behavior. This 'period range' scaling method is preferred compared to the scaling at the spectral response acceleration corresponding to the structure fundamental period to decrease the scatter in responses as suggested by previous studies (e.g. Shome et al., 1998; Martinez-Rueda, 1998; Kennedy et al., 1984).

The Regression coefficient of drift-intensity relation, b, is one of the regression coefficients for linear regression of drift demand D on the intensity S_a in logarithmic space. It can be calculated based on the regression analysis of the equation:

$$\hat{D} = a(S_a)^b \tag{5}$$

where $\hat{D}$ is the median drift demand; S_a is the spectral acceleration (measure of ground motion intensity); a and b are the regression coefficients for linear regression of drift demand D on intensity S_a in logarithmic space; a and b are the constants that control the slope and degree of nonlinearity, respectively (Aslani and Miranda, 2005). Some studies suggest $b=1.0$ for moment frames (Cornell et al., 2002; Luco and Cornell, 1998, 2000). In the present study, this parameter is found to be around 0.31 and 0.24 for FB-Conv and FB-BRB models, respectively. The COV of b is assumed in between 0.20 and 0.25. Fig. 7 shows the relation between the median drift demand $\hat{D}$ (which is represented by median maximum inter-story drift, MIDR, in the current study) and intensity S_a in a logarithmic space for FB-Conv and FB-BRB models.

The most practical way to estimate the regression parameters, a and b, is to perform nonlinear dynamic-response time-history analysis (NLTHA) on the structure using all records with scaling each record set to the corresponding intensity measure at the fundamental period of the structure. For example, for the 10-scaled records of the 200yr hazard, first nonlinear time history analyses (NLTHA) are conducted on the model structure, then the median and the standard deviation of the MIDR are obtained. This median value will be plotted against the corresponding spectral acceleration (i.e. S_a at the fundamental period of the structure). After that, one can plot the relation between the drift-demand and the intensity, and then conduct a regression analysis of ($\ln D$) on ($\ln S_a$) as shown in Fig. 7.

In records selection for NLTHA the following information is considered: the soil type, the shear wave velocity, the magnitude, the fault type, and the different distance measures from the site to the fault rupture. The records are selected from the PEER database (2013). The records are listed in the Appendix A for information and the details of these records can be found elsewhere (Nour El-Din and Kim, 2014).

The Sensitivity factor, (k/b), is an indicator of the relation between the drift, spectral acceleration, and the probability as shown in Eq. (6):

$$P_{LS}=H\left(S_a^{\hat{C}}\right)\exp\left[\frac{1}{2}\frac{k^2}{b^2}\left(\beta^2_{D|S_a}+\beta_c^2\right)\right] \tag{6}$$

where P_{LS} is the damage state probability; $S_a^{\hat{C}}$ is the spectral acceleration corresponding to the median drift capacity (obtained from drift-intensity relation Eq. (5) by setting the drift as the limit state); $H(.)$ is the seismic hazard function of spectral acceleration, the annual probability that intensity S_a at a site will equal or exceed s_a (obtained from Eq. (4)); k is one of the coefficients for linear regression of hazard $H(S_a)$ on intensity S_a in proximity of limit state probability in logarithmic space, which controls the degree of nonlinearity of the hazard curve (can be obtained from the hazard curve fitting); b is one of the regression coefficients for linear regression of drift demand D on intensity S_a in logarithmic space (can be obtained from drift-intensity curve fitting); $\beta_{D|s}$ is the dispersion measure for drift demand D at given S_a level; and β_C is the dispersion measure for drift capacity C (standard deviation of natural logarithm) assumed to be 0.3 based on previous studies (e.g. Cornell et al., 2002).

It can be observed that change in drift by x leads to a change in S_a by a factor of $x^{1/b}$, which in turn implies a change in the probability by $x^{k/b}$ (Cornell et al., 2002). The mean and the COV of this factor (k/b) will be taken based on those of k and b parameters explained in the previous sections. The sensitivity factor (k/b) has not been considered in the LHS method because it is a dependent variable (i.e. dependent on k and b variables).

4.5. Uncertainity of seismic LCC parameters

The parameters associated with the seismic LCC analysis include limit state total repair costs, initial costs, service lifetime, annual momentary discount rate, and maintenance cost. In general, there are two categories of the limit state damage cost in fixed offshore structures (Gang et al., 2009). The first is the direct limit-state damage cost, which is related to repair cost, cost of damage to equipment, cost of deferred production, death and injury losses. The second is the indirect limit-state damage cost which is related to environmental and socio-economic impacts caused by the collapse or explosion of the platform. The damage costs usually include the cost of repair, the loss of equipment, the deferred production loss, the cost of injuries, the loss associated with fatality, and the indirect losses related to the loss corresponding to platform collapse. Details about the calculation formula for each component of the limit state cost can be found elsewhere (e.g. Gang et al., 2009).

It needs to be stated that the current study focuses on repair cost only. This is because the lack of reliable data regarding the other cost items for the Gulf of Moattam. In addition, some cost items are highly variable depending on the type and function of the platform. For example, for unmanned platforms, the cost of injuries and the loss associated with fatality may not exist. In addition, the cost associated with the loss of equipment is highly dependent on the function of the platform whether it is wellhead platform, processing platform, accommodation platform, etc. Moreover, the cost of deferred production loss and indirect losses highly variable from one region to another. For example, based on Gang et al. (2009), which used Gulf of Mexico as a reference data, the deferred production loss and indirect losses may reach 100 and 3000 times the initial cost. In this case, these two cost items will dominate the total life cycle cost and the effect of other input variable will be marginal.

The limit state repair cost C_{LS}, for the ith limit state, can be formulated as follows (Gang et al., 2009):

$$C_{LS}^{i}=\begin{cases}(R_C/D_R)D_1 D_1 < D_R\\ R_C D_1 \geq D_R\end{cases} \tag{7}$$

where R_C is the replacement cost, D_1 is the damage index of the platform which can be expressed as the ratio between the actual and allowable maximum inter-story drift ratios $(D_1 = \mathrm{MIDR}_{act}/\mathrm{MIDR}_{all})$; $\mathrm{MIDR}_{all}=H/50$, where H is the vertical distance between the horizontal bracing levels in the jacket structure. D_R is the repairable damage index $(D_R=0.6MIDR_{all})$.

Three structural damage states are used such as minor (H/250), major (H/125), and collapse (H/50). If the replacement cost is assumed equal to the initial cost, these damage state costs correspond to 33, 67, and 100%, respectively, of the initial cost of the structure.

In this study, the COV for the limit state repair costs is assumed to be in the range of 0.15–0.20 (RS Means Corp, 1997; Choun and Elnashai, 2010; Lagaros et al., 2006). It should be mentioned that in addition to the cost of repair due to seismic damage, LCC generally includes other cost items such as inspection, maintenance, and operating and demolishing cost, which are not the focus of the current paper.

The initial cost, C_O, is related to the material and the labor costs for the construction of the structure. For offshore structures, more cost items should be included such as the transportation, installation costs, etc. For simplicity, it is assumed that the initial cost will be the same for both FB-BRB and FB-Conv models. That is, the cost reduction in steel tonnage of the BRB system will offset the cost increase in BRB construction and fabrication compared to the conventional bracings (Dasse, 2007).

The construction of a fixed steel offshore platform is commonly carried out in on-shore yards. This means that material and labor are very similar to those required for the fabrication of typical steel structures. Based on that, it is reasonable to use the available data for building structures. Choun and Elnashai (2010) used 0.2 as a variability in uncertainty of the replacement cost in their study for building structure. Based on that, the logarithmic standard deviation of C_O may be assumed 0.20 in the current study.

The service lifetime of most of fixed type off shore structures ranges between 20 to 35 years according to field experience. Based on that range and using normal distribution, the mean and standard deviation will be 27.5 and 7.5 years, respectively, which leads to COV=0.3. The annual momentary discount rate is used to calculate the value of benefits or costs that will occur in the future. According to FEMA 227 (1992b) and Wen and Kang (2001b), a discount rate of 3 or 4% is reasonable for public sector considerations, and for private sector considerations a slightly higher rate of 4–6% is reasonable. A discount rate is used to calculate the value of benefits or costs that will occur in the future. Increasing the discount rate lowers the present value of future benefits. Conversely, assuming a lower discount rate raises the present value of future benefits or cost. Since the current platform under consideration is owned by a national oil company of a country (i.e. public sector), 3% discount rate is used as a mean value and 0.3 is used as its COV. The variability in maintenance cost per year is assumed as the same with the variability of initial cost and limit state cost (i.e. COV=0.15 to 0.2), and the mean value is assumed to be 0.1 of the initial cost based on previous experience similar to the platform structure under consideration. The focus of the current study is on the structural maintenance cost, which will not cause shut down of the platform or stopping the operation and production.

5. Formulation of seismic LCC

The expected LCC of a structure can be calculated as follows (Wen and Kang, 2001a; Gencturk, 2013):

$$E\left[C_{LC}\right]=C_o+\int_0^L E\left[C_{SD}\right]\left(\frac{1}{1+\lambda}\right)^t dt=C_o+\alpha L E\left[C_{SD}\right] \tag{8}$$

where C_o is the initial construction cost which will be related to the material cost in the current study, L is the service life of the structure, λ is the annual discount rate, and $E[C_{SD}]$ is the annual expected seismic damage cost, which is governed by a Poisson process (implicit in hazard modeling)and does not depend on time. It is assumed that structural capacity does not degrade over time and the structure is restored to its original condition after each hazard; On the right hand side, α is the discount factor which is equal to $[1\text{-}\exp(-ql)]/ql$, where $q = \ln(1+\lambda)$. $E[C_{SD}]$ is given by

$$E\left[C_{SD}\right]=\sum_{i=1}^{N} C_i P_i \tag{9}$$

where N is the total number of limit-states considered, $_{Pi}$ is the total probability that the structure is in the ith damage state throughout its lifetime, and C_i is the corresponding cost. In accordance with the definition of seismic hazard, three structural damage states are used (i.e. N is equal to three) such as IO, LS, and CP, and C_i is assumed to be 30, 70, and 100 percent, respectively, of the initial cost of the structure. This is based on the correspondence of these damage states with the information provided by Gang et al. (2009) which is similar to building structures as provided by Fragiadakis et al. (2006). Unlike TDA and FOSM, the C_{ls} variable is considered independent of the initial cost in the LCC calculation using the LHS method. However, the same upper and lower bounds used in the TDA and FOSM methods are used for the stratification of the variable in the LHS method. This is to achieve a common base of comparison among the three methods for this particular variable. $_{Pi}$ is given by

$$P_i=P\left(\Delta_D > \Delta_{C,i}\right)-P\left(\Delta_D > \Delta_{C,i+1}\right) \tag{10}$$

where Δ_D is the earthquake demand and $\Delta_{C,i}$ is the structural capacity, usually represented in terms of drift ratio, defining the ith damage state. The probability of demand being greater than capacity, $\Delta_D > \Delta_{C,i}$, is evaluated as discussed in Section 4.4 using Eq. (6)

Table 4
The best estimate values and COV of the loss estimation and LCC variables of the base-case.

Parameter	FB-Conv			FB-BRB			COV[a]	Note
Limit state	L_{S1}	L_{S2}	L_{S3}	L_{S1}	L_{S2}	L_{S3}	-	
MIDR, %	1	2	3	1	2	3	–	% of Jacket height
L, (years)	30			30			0.30	
$S_a^{\hat{c}}$, g	0.30	0.52	0.63	0.45	0.66	0.78	0.50	
$\beta_{D\mid Sa}$	0.3			0.3			0.30	
k_o	1.48E-04			8.35E-05			–	
k	1.80			1.63			0.20	
b	0.312			0.24			0.25	
β_C	0.3			0.3			0.30	
C_o,$	28,900			28,900			0.2	Assuming initial cost is the same for conventional brace and BRB
C_i,$	8,670	14,450	20,230	8,670	14,450	20,230	0.2	Assuming 0.3, 0.5, and 0.7 of C_o,respectively
λ	0.03			0.03			0.3	
C_m	2,890			2,890			0.2	Assuming 0.1 of C_o.
Sensitivity factor (k/b)	5.77			6.79			0.2–0.25	

[a] All variables are assumed normally distributed with mean bias = 1.0.

6. Sensitivity analysis of seismic LCC

In this section, the sensitivity of seismic LCC for various uncertain input parameters is investigated. Through the sensitivity study, the expected ranges of LCC variation can be identified. Statistical data available for offshore structures in literatures are used in the analysis, but some data not available in the literature are determined based on practical experience and engineering judgement. The sensitivity analysis used in this study involves comparisons of the results determined from the deterministic model. The results of the sensitivity analysis are used in order to rank the random variables by their impact on the seismic LCC. The variation of the LCC estimations obtained from three different analysis methods such as TDA, FOSM, and the LHS methods are compared to ensure the reliability of the results. The FB-Conv and FB-BRB cases with pile end condition are used as case study structures for this sensitivity analysis. All variables are set to their best estimate (i.e. mean value) in the base case model, then, the LCC is estimated for the upper and lower bounds of each input variable using TDA, FOSM, or LHS methods. Table 4 shows the best estimate values (i.e. mean) of the loss estimation and LCC variables of the base-case.

6.1. Variation of seismic hazard and demand-intensity relation

Structural modeling variables such as damping, plastic hinge property, mass, soil-pile friction, etc., have direct impact on the seismic hazard and the demand-intensity relation through the k and b parameters. That is, the variability in LCC due to variability in structural modeling variables is controlled through k and b parameters. Figs. 8 and 9 show the variability of the seismic hazard due to variability in damping and mass in FB-Conv and FB-BRB models, respectively.

The variation in damping ratio is defined in Fig. 8 using the 10th and the 90th percentiles of the lognormal distribution as the lower and the upper bounds, respectively. In this case, the mean and the standard deviation of the damping ratio are logarithmically transformed to be 1.535 and 0.385, respectively. Using the inverse of the lognormal distribution, the lower and the upper bounds of the damping ratio become 2.8% and 7.6%, respectively. As can be observed in Fig. 8, the spectral acceleration values of the 10th percentile trend line are larger compared to those of the 90th percentile values for the same annual frequency of exceedance. This is because the response spectrum associated with the lower bound damping ratio shifted up, which results in larger spectral acceleration associated with the same natural period of the structure.

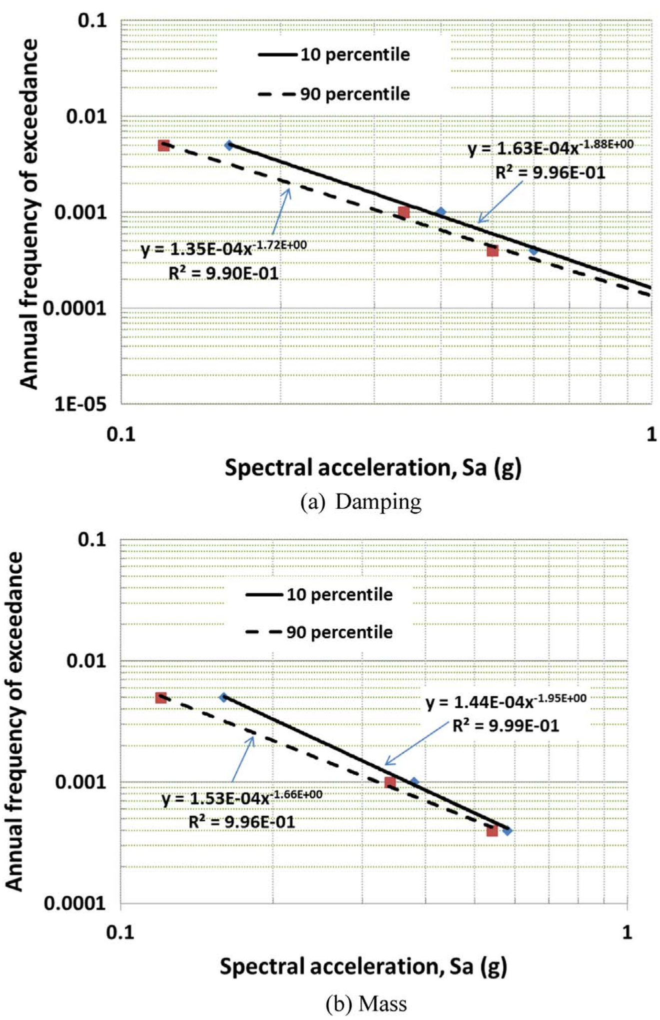

Fig. 8. Variability in seismic hazard of FB-Conv model due to variability in (a) damping and (b) mass.

In Fig. 9, the variation in mass is calculated using the 10th and the 90th percentiles of the Gaussian distribution as the lower and the upper bounds, respectively. In this case, mass is varied

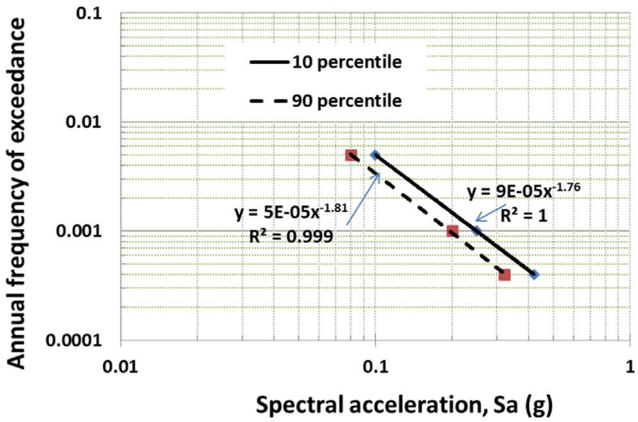

(a) Damping

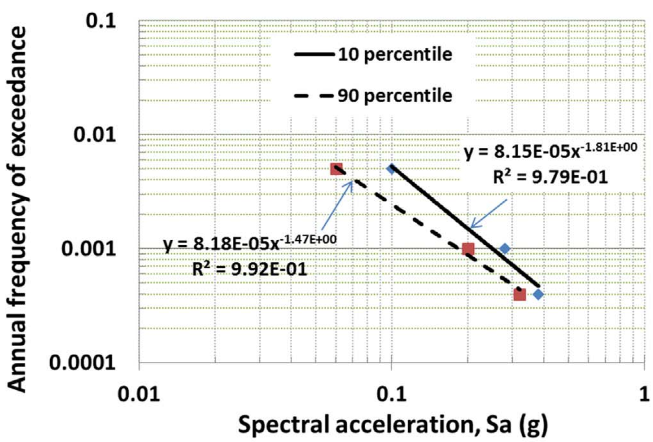

(b) Mass

Fig. 9. Variability in seismic hazard of FB-BRB model due to variability in (a) damping and (b) mass.

between 0.923M and 1.077M , where M refers to the mean dead load mass, and the factors 0.923 and 1.077 refer to the inverse of a Gaussian distribution with unit mean and coefficient of variation of 0.06, evaluated at the 10th and the 90th percentiles, respectively. It can be observed in Fig. 9 that the spectral acceleration values of the 10th percentile trend line are larger compared to those of the 90th percentile values for the same annual frequency of exceedance. This can be attributed to the reduction of the natural period of the structure when the lower bound mass is used. This reduction in structure natural period increases the corresponding spectral acceleration for the same annual frequency of exceedance.

Figs. 10 and 11 present the variability of the demand-intensity relation due to the variability in damping, plastic hinge property, mass, and soil-pile friction parameters in FB-Conv and FB-BRB models, respectively. The variabilities in damping and mass will be similar to those of the FB-Conv model as discussed above. Variability in the resistance of the plastic hinge follows an approach called ‘random strength, constant stiffness’ which was recommended by Porter et al. (2002). In this approach, every force and deformation value on the force-deformation relationship is scaled by a single, random variable. In this case, strength is varied between 0.74F and 1.26F, where F refers to the mean nominal strength of the element under consideration, and the factors 0.74 and 1.26 are the inverse of a Gaussian distribution with unit mean and coefficient of variation of 0.20, evaluated at the 10th and the 90th percentiles, respectively. In a similar fashion, the lower and the upper bounds of soil friction resistance are found to be 0.76F and 1.24F, respectively, where F refers to the mean nominal strength of the soil friction.

As can be observed in Figs. 10 and 11, the degree of non-linearity, which is controlled by the factor b, is larger in the case of FB-Conv compared to that of the FB-BRB. This may be justified based on the behavior of each system in the nonlinear range, where ductility plays an important role. FB-BRB, which is more ductile, shows less variation of the mean responses of the structure with changes in the level of ground motion intensity. Another interesting observation is that in the case of damping and mass variables, the difference between the b values of the 10th and the 90th percentiles for FB-BRB is almost double that of the FB-Conv. However, in the case of the soil-pile friction variable, this difference is almost in the same order of magnitude. Bearing in mind that the increase in b leads to decrease in the probability of a damage state as given by Eq. (6), this observation may be useful for predicting and justifying the relative LCC swing of these variables. That is, it is expected that the LCC swings associated with the FB-Conv, for damping and mass variables, are larger than their counter parts in the FB-BRB case. However, for the soil-pile friction variable, the same LCC swing is expected for both FB-Conv and FB-BRB.

6.2. LCC sensitivity

For explanation purpose, an example based on TDA method is detailed in this section. Table 5 shows summary of the LCC estimation for FB-Conv model considering variability of various design variables. In TDA, it is assumed that the output variable (EDP, which is the LCC estimation in this study) is a known deterministic function of a set of input variables whose probability distribution is described in Tables 2 and 3. For each input variable, the best estimate (mean value) and two extreme values corresponding to upper and lower bounds (which are 10th and 90th percentiles in this study) of its probability distribution are selected. For damping variable, as in example, these values are 2.83%, 7.6%, 5.0% for lower bound, upper bound, and mean, respectively.

First, using SAP2000 software, an FEM model is built using input variables set to their best estimates (i.e mean value) and the fundamental period is obtained (fundamental period, T_n=1.8 s for FB-Conv Model). After that, the hazard curve is plotted at period equal to the fundamental period of the model under investigation (as shown in Fig. 6a). The three points on the hazard curve represent the three different spectral acceleration corresponding to the selected hazards (200, 1000, and 2475 years) at T_n=1.8 s. Theses spectral accelerations are extracted from the corresponding response spectra at 5.0% damping (i.e. at the mean value). Using hazard curve fitting, the coefficient k is obtained (k=1.8 as shown in Table 4 for FB-Conv). This is considered as the mean value of this input variable, which is used for the base case. Subsequently, for this input variable, the value is evaluated twice, using one of the extreme values of damping ratio each time while the other input variables are set to be their best estimates (i.e. mean value). This process yields two bounding values of the coefficient k, which are 1.9 and 1.7 for the lower and the upper bounds, respectively, as shown in Table 5. After that, the demand-intensity relation is plotted through NLTHA using three sets of earthquake records given in the Appendix A. Each set of records corresponds to a hazard level. For each set, the median MIDR is calculated and plotted against the corresponding spectral acceleration at the fundamental period of the structure using 5.0% damping ratio. From this plot, the coefficient b is obtained (b=0.312 as shown in Table 4 for FB-Conv). The standard deviation of the MIDR at this stage will be used later as the dispersion measure ($\beta_{D|s}$) for the drift demand D at given S_a level.

Using the mean of all input variable, the demand-intensity

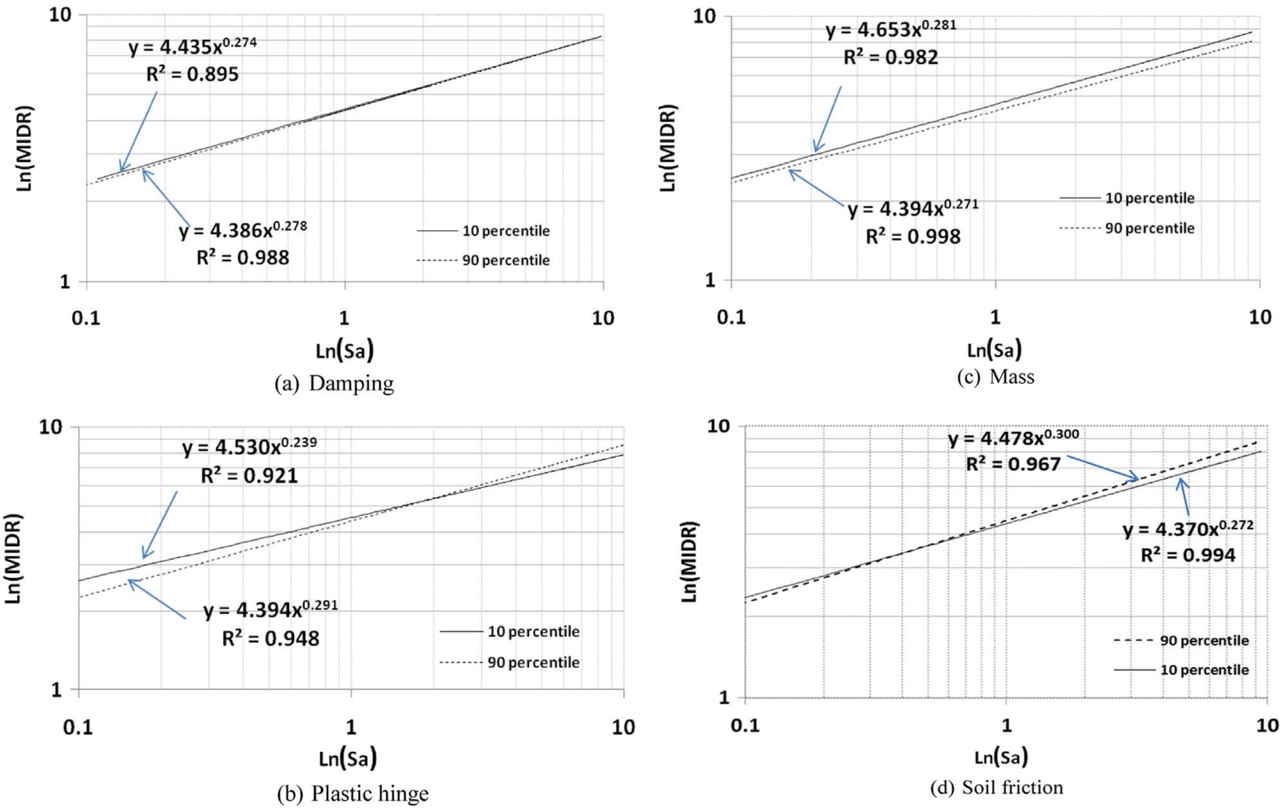

Fig. 10. Variability in the relation between drift demand *(MIDR)* and intensity (S_a) for FB-Conv due to variability in various parameter.

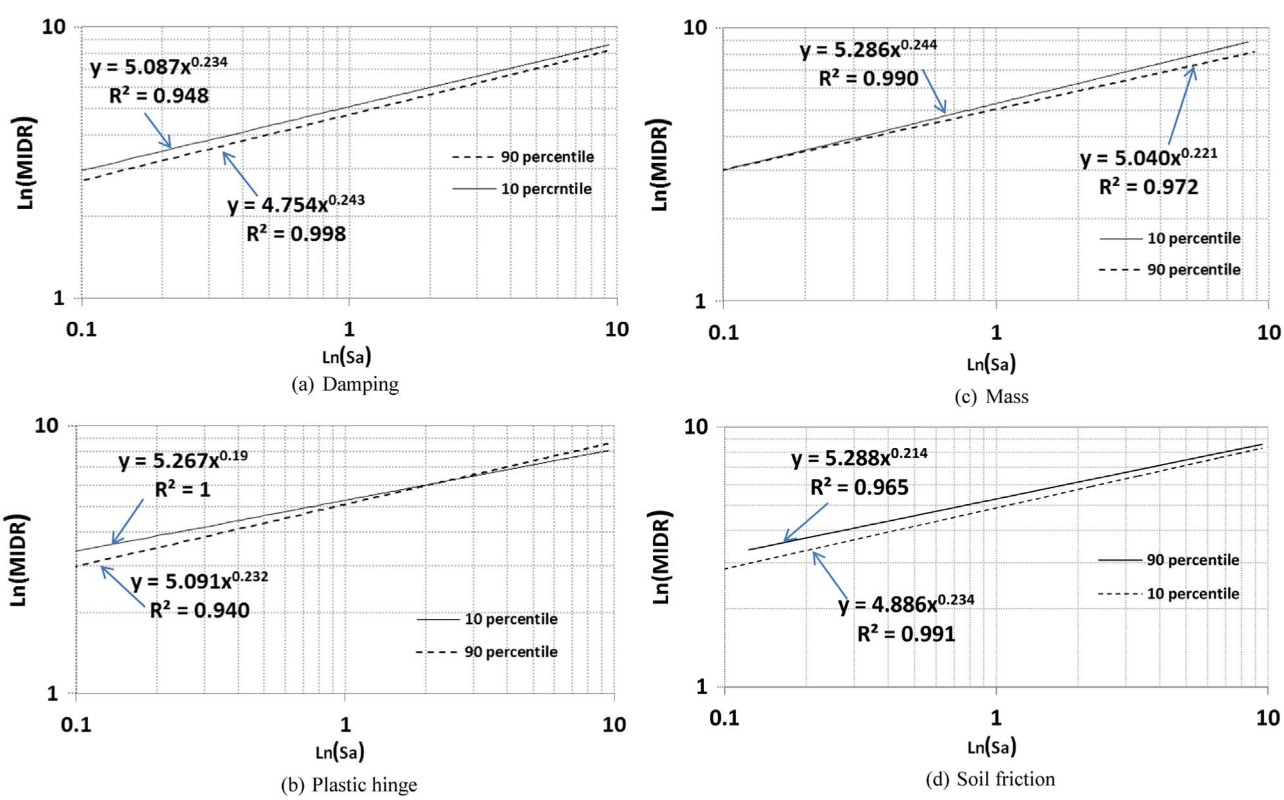

Fig. 11. Variability in the relation between drift demand (MIDR) and intensity (S_a) for FB-BRB due to variability in various parameters.

relation is plotted as shown in Fig. 7. The same process will be repeated for the 2.83% and 7.6% damping ratios and the corresponding lower and upper bounds of the coefficient b are found to be 0.274 and 0.278, respectively, as shown in Table 5 and Fig. 10a. From demand-intensity relation and using the limit-state values (i.e. immediate occupancy (IO), life safety (LS), and collapse

Table 5
Parameters used for LCC estimation of FB-Conv model considering variability of various design variables.

(a) Damping ratio variability							
Parameter	FB-Conv ($\zeta_{10\%}$)			FB-Conv($\zeta_{90\%}$)			Note
Limit state	L_{S1}	L_{S2}	L_{S3}	L_{S1}	L_{S2}	L_{S3}	
MIDR, %	1	2	3	1	2	3	% of Jacket height
$S_a^{\hat{c}}$, g	0.30	0.55	0.67	0.5	0.73	0.80	
$H(s_a)$	0.00163	0.00051	0.00035	0.00046	0.00024	0.00020	
k_o	1.63E-04			1.35E-04			
k	1.9			1.7			
b	0.274			0.278			
$P(LS_{\vert Sa})$, %	12.9	4.05	2.78	1.77	0.905	0.77	at $S_a^{\hat{c}}$
P_i,%	8.84	1.27	2.78	0.863	0.135	0.77	
LCC, $	58,978			33,876			
(b) Plastic hinge variability							
$S_a^{\hat{c}}$, g	0.30	0.55	0.67	0.30	0.55	0.67	
$H(s_a)$	0.00129	0.00043	0.00030	0.00129	0.00043	0.00030	
k_o	1.48E-04			1.48E-04			
k	1.8			1.8			
b	0.24			0.291			
$P(LS_{\vert Sa})$, %	20.4	6.85	4.8	4.045	1.356	0.952	at $S_a^{\hat{c}}$
P_i,%	13.56	2.051	4.8	2.69	0.406	0.952	
LCC, $	77,533			38,534			
(c) Mass variability							
$S_a^{\hat{c}}$, g	0.37	0.55	0.69	0.30	0.53	0.64	
$H(s_a)$	0.00100	0.00048	0.00030	0.00113	0.00044	0.00032	
k_o	1.44E-04			1.53E-04			
k	1.95			1.66			
b	0.281			0.271			
$P(LS_{\vert Sa})$, %	7.6	3.52	2.26	3.306	1.285	0.940	at $S_a^{\hat{c}}$
P_i,%	4.1	1.26	2.26	2.02	0.345	0.940	
LCC, $	48,718			37,159			
(d) Soil-pile friction variability							
$S_a^{\hat{c}}$, g	0.30	0.55	0.67	0.30	0.55	0.67	
$H(s_a)$	0.00129	0.00043	0.00030	0.00129	0.00043	0.00030	
k_o	1.48E-04			1.48E-04			
k	1.8			1.8			
b	0.272			0.3			
$P(LS_{\vert Sa})$, %	6.65	2.235	1.57	3.3	1.1	0.78	at $S_a^{\hat{c}}$
P_i,%	4.42	0.67	1.57	2.19	0.331	0.78	
LCC, $	36,760			44,750			

prevention (CP) limit states), one can read across the plot to obtain the corresponding capacity spectral acceleration ($S_a^{\hat{c}}$) for each limit state as shown in Tables 4 and 5. This will be repeated for the lower and upper bounds of the damping ratio. The corresponding $H\left(S_a^{\hat{c}}\right)$, as given in Table 5 for each limit state, can be obtained from Fig. 8 or Eq. (4). After that, damage state probability (P_{LS}) is calculated from Eq. (6) for the lower and upper bounds of the damping ratio. Finally, LCC is estimated using Eq. (8) for the lower and upper bounds of variable. The absolute difference of these two values, referred to as the *swing* and is illustrated in Fig. 12, is used as an indicator of the significance of the given input variable to the output variable. In Fig. 12, the input variables are ranked according to their swings. A larger swing implies a more significant input variable to the uncertainty of the LCC estimation.

It is worthwhile to mention that in TDA and FOSM, each variable has one value (10th percentile or 90th percentile) and all remaining variables are set to be their mean. If there is a dependency between two variables, the value of the dependent variable will be changed naturally due to the independent variable in the same simulation. In LHS method, for the same simulation, all variables should have a specific value based on the stratification of each variable. Based on that, the dependent variable should be set to a specific value; however, this value will be changed during the simulation due to the independent variable. This means that the dependent variable will have two values in the same simulation, which is impossible. Consequently, this requires division of variables into three sets based on their dependency.

For the LHS method, three variable sets are used for the simulation as shown in Table 6. This division is made because Set (2) and (3) variables are dependent on the Set (1) variables. This means that the change in any variable from Set (1) will result in change in Set (2) and (3) variables. Similarly, Set (3) is dependent on Set (2). Based on that, two matrices of ranking coefficients $[R1]_{9x18}$and $[R2]_{5x10}$ are utilized with corresponding correlation matrices $[S1]_{9x18}$ and $[S2]_{5x10}$. $[R1]_{9x18}$ and $[S1]_{9x18}$ matrices are associated with the nine variables in set (1). $[R2]_{5x10}$ and $[S2]_{5x10}$ matrices are associated with the five variables in Set (2) and (3). The Matlab programming code is used to achieve a reasonable norm (E) to have common basis for comparison. The maximum individual norm (E_{max}) is 0.048 and 0.013, respectively, for E_{1max} and E_{2max}. The overall norm, $E_{overall}$, obtained from Eq. (1) is 0.003

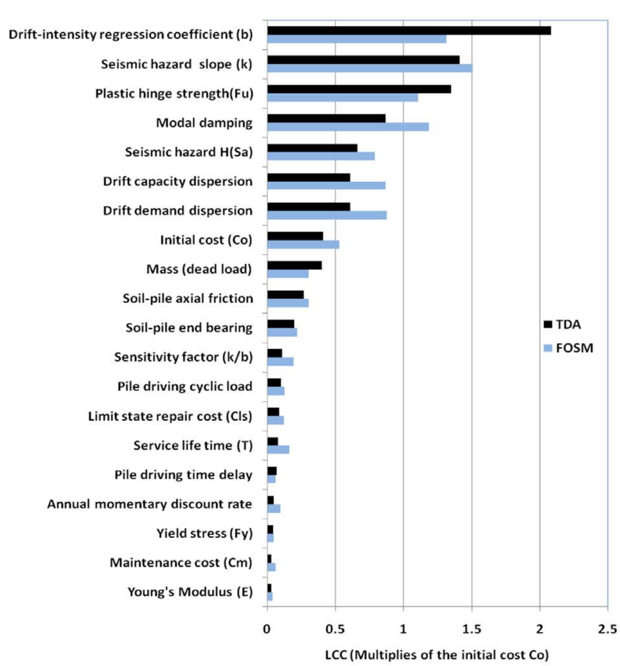

(a) FB-Conv

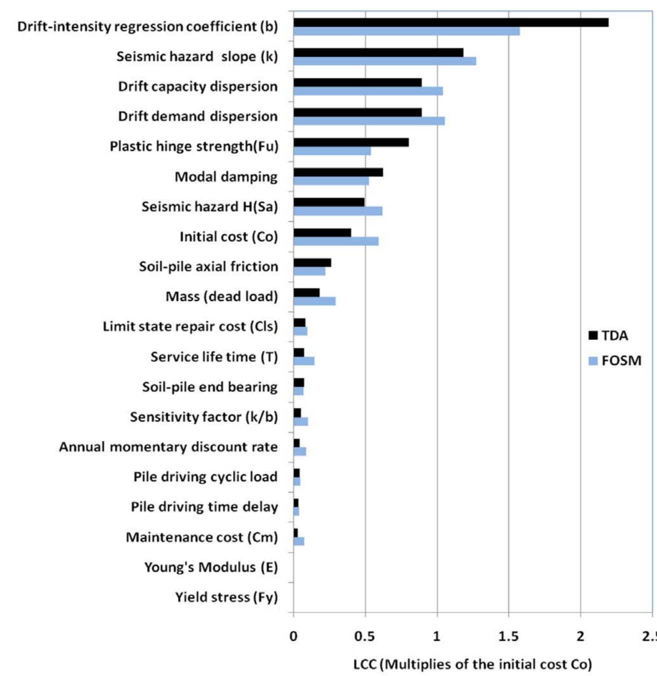

(b) FB-BRB

Fig. 12. LCC sensitivity to all LCC variables obtained using TDA and FOSM methods.

Table 6.
The Spearman rank-order correlation coefficient (ρ_i) for all input variables.

No.	Variables	The Spearman rank-order correlation coefficient (ρ_i)		Input variable category	Remark
		FB-Conv.	FB-BRB		
1	Mass (Dead load)	0.56	0.57	Structural modeling and SPSI input variables	Variable set (1)
2	Yield stress (F_y)	0.14	0.11		
3	Young's modulus (E)	0.09	0.00		
4	Modal damping ratio	0.58	0.60		
5	Plastic hinge property strength (F_u)	0.800	0.62		
6	Soil-Pile Axial Friction, ($X_{friction}$)	0.51	0.46		
7	Soil-Pile End Bearing, ($X_{bearing}$)	0.05	0.03		
8	Pile Driving Cyclic Load, (X_{cyclic})	0.01	0.03		
9	Pile Driving Time Delay, (X_{delay})	0.01	0.08		
10	Seismic hazard slope (k)	0.72	0.73	Seismic and Loss estimation input variables	Variable set (2)
11	Drift-intensity regression coefficient (b)	0.92	0.91		
12	Spectral acceleration (S_a)	0.85	0.83		
13	Drift capacity dispersion (β_{Dls})	0.69	0.66		
14	Drift demand dispersion (β_C)	0.66	0.65		
15	Sensitivity factor (k/b)[a]	–	–		
16	Initial cost (C_o)	0.67	0.80	Cost-related input variables	Variable set (3)
17	Limit state repair cost (C_{ls})[b]	0.77	0.74		
18	Service life time (T)	0.080	0.078		
19	Annual momentary discount rate	0.084	0.087		
20	Maintenance cost (C_m)	0.079	0.070		

[a] This factor is dependent variable, so it cannot be simulated in the LHS method.
[b] This variable has been considered independent of the initial cost in the LHS simulations.

and 0.079, respectively, for $[S1]_{9x18}$ and $[S2]_{5x10}$.

6.3. LCC sensitivity swing

Fig. 12 shows the sensitivity of LCC due to all variables using TDA and FOSM methods and Fig. 13 shows the sensitivity for the LHS method. The discussion of the results based on variables source can be summarized as follows,

- **Structural modeling and SPSI uncertain variables**
  Among the structural capacity and modeling uncertain variables, the modal damping ratio and the plastic hinge strength turn out to have the most significant effect on the variability of LCC according to the results of the TDA and FOSM methods. Similar trend is observed in case of using the LHS method as shown in Fig. 13. In addition, the figures show that LCC swing is larger in case of the FB-Conv structure compared to the FB-BRB case for most structural modeling and SPSI variables. This implies that the effect of these variables is much higher in case of using conventional bracing. The large LCC swing associated with the modal damping ratio can be attributed to the high COV value of this variable, which is 40%. On the other hand, the large swing associated with the plastic hinge strength shows that this variable is highly correlated with the structural global strength

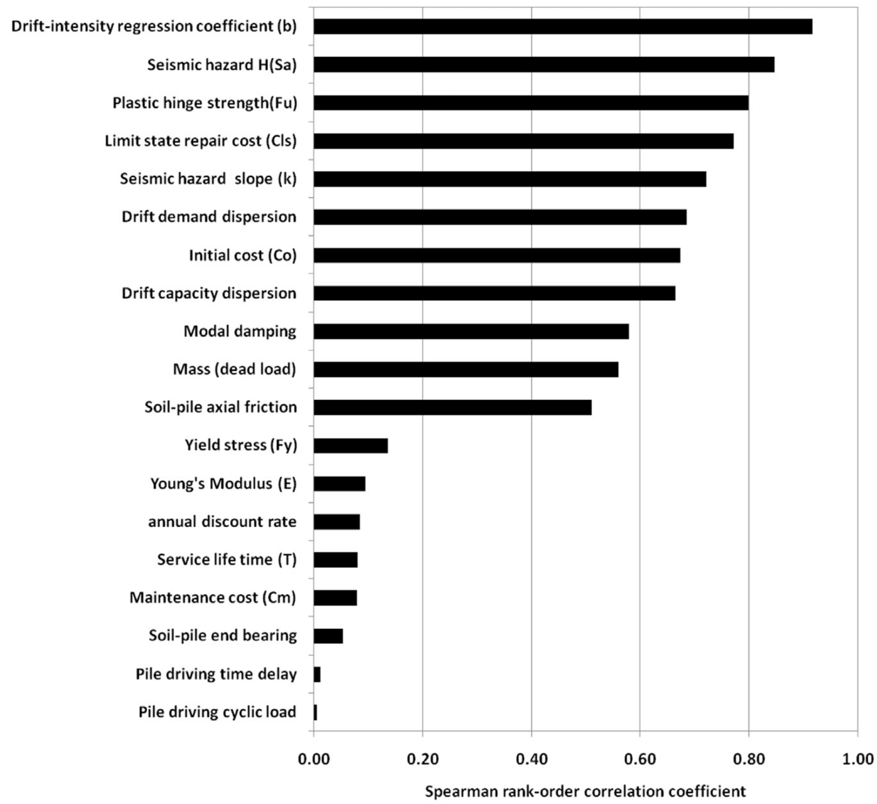

(a) FB-Conv

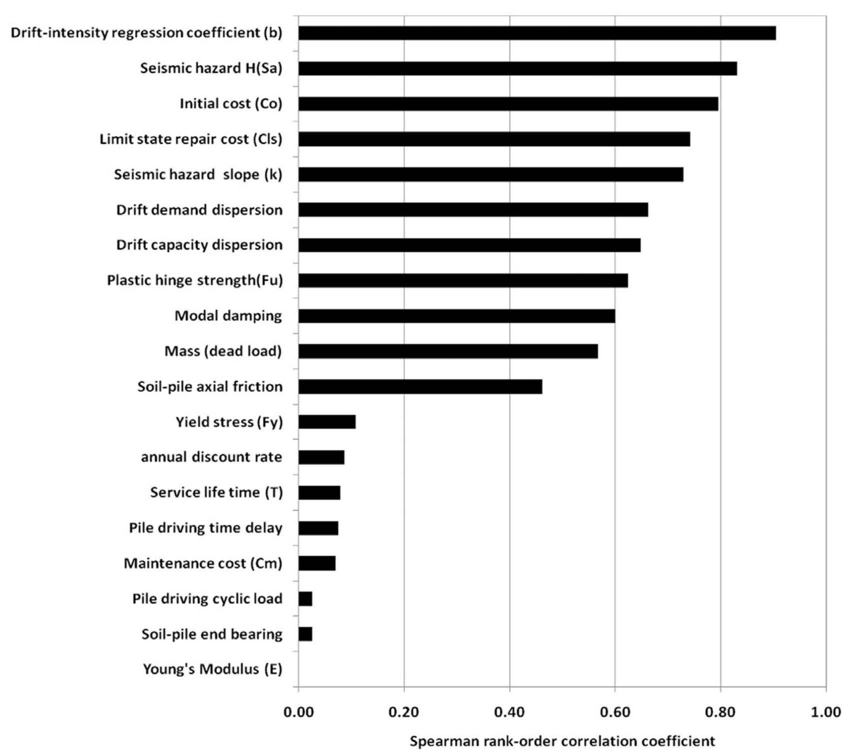

(b) FB-BRB

Fig. 13. Spearman rank-order correlation coefficient (ρ_i) for all input variables.

as well as the maximum deformation capacity. It also can be observed from the figures that variables such as F_y and E impose little influence on the LCC in case of FB-Conv and no effect in case of FB-BRB. This observation has been reported in previous studies (e.g. Jeong and Elnashai, 2007; Lee and Mosalam, 2005). This can be explained by the fact that the mean capacity of a structure is only slightly affected by the material randomness, which is an unbiased normal distribution around the mean material properties. In addition, the effect of material randomness on the response variation is overshadowed by the randomness in the earthquake record set. The latter conclusion has been reported in other studies (e.g. Wenet al., 2004; Pinto et al., 2004; Kwon and Elnashai, 2006).

The pile driving cyclic load, X_{cyclic}, and pile driving time delay, X_{delay}, have little effect on LCC variability in the case of FB-BRB and have modest influence in the FB-Conv as shown in Fig. 12. On the other hand, $X_{friction}$ and $X_{bearing}$ show moderate effect on the LCC variability in both models. This proves that SPSI modeling variables turn out to have much less impact on the sensitivity of LCC compared with the parameters associated with structural modeling. This finding is backed-up by the results of the LHS method as shown in Fig. 13.

- **Loss-estimation and seismic hazard variables**

For loss-estimation and seismic hazard variables, it can be observed from Fig. 12 that the drift-intensity regression factor (b) has the highest influence on LCC in both model structures. This reflects the significance of the structural system response to the selected intensity measure on the LCC estimation. The second highest effect (among loss-estimation and seismic hazard variables) on the LCC swing results from the seismic hazard slope (k),then follow the seismic hazard $H(S_a)$ and the dispersion in capacity and demand for FB-Conv. The significant impact of hazard function variability appears to be attributable to the inherent record-to-record variability of the ground motion profiles. The drift capacity and demand dispersions show moderate effect on the LCC with larger swing in FB-BRB compared to FB-Conv. This can be attributed to the bigger difference between the upper and lower bounds in the probability of exceeding the limit states, e.g. P_{PL}(IO), in FB-BRB compared to the FB-Conv case. The sensitivity factor (k/b) shows modest effect on the LCC swings, which is attributed to the opposite effect of the parameters b and k on LCC; the increase of k value leads to decrease in the LCC estimation, whereas the opposite is true for b.

It is found that the sensitivity swings for some of the uncertain parameters such as k and S_a of the FB-BRB model are smaller than those for the FB-Conv case. This is due mostly to the different seismic responses of the models. For low levels of seismic intensity, the responses of the models are controlled by the elastic stiffness of the models, where the stiffer FB-Conv model shows smaller MIDR compared to the more ductile FB-BRB. This increases the probability of exceedance of the limit state; consequently, the annual probability of exceedance of hazard increases leading to higher LCC swings. On the other hand, for seismic loads with high intensity, the models are controlled by the inelastic response, and the FB-Conv shows larger MIDR compared to the more ductile FB-BRB model. Consequently, the hazard annual probability of exceedance of the FB-BRB decreases leading to lower LCC swings. Fig. 13 shows the results of the LHS method, where b factor shows the highest ρ_i followed by S_a and k (among loss-estimation and seismic hazard variables) then the remaining variables. The sensitivity factor (k/b) is not simulated since it is a dependent variable on b and k.

It has been observed that the higher the natural period of the structures becomes, the lower the LCC swings of most parameters become. This can be attributed to the higher seismic intensity corresponding with the lower natural periods of the models. In addition, it is found that when the value of the factor k, which controls the degree of non-linearity of the hazard function, is higher than 1.9, the LCC swings increase significantly.

- **Cost and service lifetime variables**

Generally, the initial cost plays an important role in the LCC variability not only because it has a direct effect on estimating LCC but also because the cost of exceedance of all limit states is taken as a percentage of the initial cost. As can be observed from Fig. 12, the LCC swing associated with the initial cost is similar in the FB-Conv with that in the FB-BRB. This is due to the assumption that the initial cost is the same for FB-Conv and FB-BRB as explained before. The other parameters are found to be bounded by 0.2 C_o limit in both model cases. The LCC sensitivity found to be affected little from the maintenance cost and annual momentary discount rate in both models. In the LHS method, the ρ_i associated with C_o and C_{LS} are similar as indicated in Fig. 13. This may be due to the un-coupling assumption made between variables C_o and C_{LS}. This assumption reduces the effect of C_o on LCC compared to C_{LS}.

7. General discussion

Generally, the relative importance of the variables obtained from the three sensitivity methods is not expected to be identical, especially in the case of LHS method where the number of simulations and the number of input variable play important role in the results. In addition, for LHS method, some input variables (such as structural modeling variables) are dependent on other variables (such as seismic hazard and the demand-intensity relation variables). This leads to division of the variables into three sets with two matrices of ranking coefficients. Consequently, this makes the norm E for one group of variable different from the others, which have an impact on the results. As can be observed in Figs. 12 and 13, the greatest part of the LCC uncertainty is due to the uncertainty in the drift-intensity relation regression coefficient b. This may be reduced, partially, by the additional knowledge of structural response and seismic hazard, but is still disturbed by the aleatory uncertainty in the nature of the seismic hazard and the future earthquakes. The figures suggest that uncertainty in the variables that affect the response, such as modal damping and plastic hinge strength, have relatively moderate contribution to the LCC uncertainty. That is, these variables directly reflect the structural response without the intervention of the aleatory uncertainty associated with earthquake intensity or profile. The seismic hazard slope k is found to have the second highest influence on the LCC uncertainty for both FB-Conv and FB-BRB. Modal damping and plastic hinge strength prove to play more important role in the LCC uncertainty in the case of FB-Conv. This can be attributed to the large impact of these variables in the non-linear range where the variability in the global response produces large demand dispersions that lead to more variations in the LCC estimations. However, dispersion in demand and capacity found to have, relatively, higher effect in case of FB-BRB when compared to the effect of plastic hinge and damping. Other variables such as pile driving time delay and the pile driving cyclic load turn out to have modest impact on the LCC estimation. In the FB-BRB case, the yield stress and Young's modulus have almost no effect on the LCC estimation.

In the sensitivity analysis process, it is observed that some variables have significant effect if they are uncoupled with other variables; however, their effect becomes marginal in case they are coupled with these variables. For example, the b and k variables show large LCC swings, but when they are coupled, their effect is insignificant as can be observed in the LCC swing associated with the sensitivity factor k/b. Some variables, such as $\beta_{D|S_a}$ and β_C, are dependent on the selection of the hazard records as well as the response of the structures to these records intensities and profiles. This means that they are highly affected by the variability in the selected earthquake records. It is found that as the variability in the selected hazard (intensity and profile) decreases, the contribution of these factors to the LCC variability also decreases.

The effect of some variables on LCC is filtered out by the probability of exceedance associated with the hazard level used. For example, even if the limit state cost variable C_{LS} for the life safety (LS) and collapse prevention (CP) limit states is much higher than that of the immediate occupancy (IO) limit state, its effect fades away because of the low probability of exceedance associated with the former limit states. For example when mass variable is maintained at its lower bound, i.e. 10 percentile, as shown in Table 5(c), and the remaining input variables are maintained to their best estimates in case of FB-Conv model, P_{PL}(IO) equals to 7.60%.However, this percentage is found to be 3.52% and 2.26% for P_{PL}(LS) and P_{PL}(CP), respectively. In the FB-BRB case, P_{PL}(IO) equals to 2.66% and the P_{PL}(LS) and P_{PL}(CP) values are found to be 1.51% and 1.4%, respectively.

8. Summary and conclusion

In this study, the sensitivity of various uncertain input parameters for seismic LCC evaluation of offshore platform was investigated using various methods such as Tornado Diagram Analysis (TDA), First-Order Second Moment (FOSM), and Latin Hypercube Sampling (LHS) methods.

The analysis results showed that the uncertainties associated with the soil-pile have modest effect on the LCC estimation of the fixed type steel offshore platform. $X_{friction}$ proved to be the most important uncertain parameter among the soil-pile modeling parameters. Among the structural uncertain parameters, the variability in plastic hinge strength and damping ratio had the most significant impact on the LCC, whereas the mass showed relatively moderate effect. Elastic modulus, and yield stress showed marginal effects on the LCC estimations. In the loss estimation and seismic hazard uncertain variables, the coefficient b had a more dominant influence on the LCC variability compared to the other variables. The seismic hazard slope k variability showed a high influence on the LCC variability. Seismic hazard, drift capacity dispersion, and drift demand dispersion had moderate effect with LCC swings around (0.5–1.0) C_o. The initial cost proved to have the most influential effect among the different cost items of LCC estimation.

The LCC was found to be particularly sensitive to the variability in the relation between the drift demand and hazard intensity. Therefore, potential variation in both hazard intensity and drift demand are critical considerations for LCC estimation for the structures considered in the current study. Moreover, the uncertainties associated with this relation tend to overshadow those associated with other modeling parameters, such as soil-pile modeling parameters, yield stress, Young's modulus, etc. In addition, the probability of exceeding a certain limit state plays a crucial role in reflecting the effect of many variables in the LCC estimation. Careful definition of the important variables, such as seismic hazard slope k and coefficient b, in the preliminary design stage of the structure can be critical for adequate estimation of the total LCC of fixed steel offshore platform structures used in the current study.

Finally it needs to be mentioned that some statistical data for offshore structures used in this study were obtained from general steel structures or from engineering judgements because they were not available in the literature. The validity of the present study will be enhanced if more knowledge base for offshore structures is accumulated.

Appendix A

See Table A1.

Table A1.
Characteristics of the ground motion suit used in the current study.

NGA#[a]	Event	Mag.	R_{jb}[b] (km)	R_{rup}[c] (km)
1785	Hector Mine	7.13	54.7	54.7
862	Landers	7.28	54.2	54.2
1153	Kocaeli- Turkey	7.51	126	127
1800	Hector Mine	7.13	186.8	186.8
835	Landers	7.28	135.2	135.2
1163	Kocaeli- Turkey	7.51	58.3	60
879	Landers	7.28	2.2	2.2
1604	Duzce- Turkey	7.14	182.8	183.6
833	Landers	7.28	144.9	144.9
12	Kern County	7.36	114.6	117.8
1636	Manjil- Iran	7.37	50	50
1638	Manjil- Iran	7.37	174.6	174.6
1805	Hector Mine	7.13	185	185
853	Landers	7.28	135.9	135.9
1833	Hector Mine	7.13	72.9	72.9
1602	Duzce- Turkey	7.14	12	12
1148	Kocaeli- Turkey	7.51	10.6	13.5
1799	Hector Mine	7.13	179.3	179.3
892	Landers	7.28	163.5	163.5
886	Landers	7.28	94.5	94.5
1776	Hector Mine	7.13	56.4	56.4
897	Landers	7.28	41.4	41.4
1811	Hector Mine	7.13	91.2	91.2
841	Landers	7.28	89.7	89.7
889	Landers	7.28	141.9	141.9
1167	Kocaeli- Turkey	7.51	145.1	145.1
1634	Manjil- Iran	7.37	75.6	75.6
861	Landers	7.28	156	156
1168	Kocaeli- Turkey	7.51	293.4	293.4
1759	Hector Mine	7.13	176.6	176.6

[a] Next Generation of Ground-Motion Attenuation Models.
[b] Joyner-Boore distance (km)": the horizontal distance to the surface projection of the rupture plane.
[c] Closest distance (km) to the fault rupture plane.

References

Anagnostopoulos, S.A., 1983. Pile foundation modelling for inelastic earthquake analyses of large structures. Eng. Struct. 5, P215–P222.
Ang, A.H.S., Lee, J.C., 2001. Cost optimal design of RC buildings. Reliab. Eng. Syst. Saf. 73, 233–238.
Ang, A.H.S., Tang, W.H., 2007. second ed.Probability Concepts in Engineering: Emphasis on Applications to Civil and Environmental Engineering v. 1. John Wiley & sons incorporation, New Jersey, US.
API, 2000. American Petroleum Institute Recommended Practice for Planning, Design and Constructing Fixed Offshore Platforms, 21st ed. API RP-2A, Washington.
ASCE-7 (2013), American Society for Civil Engineers. Minimum Design Loads for Buildings and Other Structures, Virginia, U.S.A.
Aslani, H., Miranda, E., 2005. Probability-based seismic response analysis. Eng. Struct. 27 (8), 151–1163. http://dx.doi.org/10.1016/j. engstruct.2005.02.015.
Baker, J.W., Cornell, C.A., 2008. Uncertainty propagation in probabilistic seismic loss estimation. Struct. Saf. 30, 236–252.
Baker, J. W., Cornell, C. A. (2003). Uncertainty specification and propagation for loss estimation using FOSM methods. In: Proceedings of the Ninth International Conference on Applications of Statistics and Probability in Civil Engineering ICASP9. San Francisco. CA.669–676.
Barbato, M., Gu, Q., Conte, J.P., 2010. Probabilistic push-over analysis of structural and soil-structure systems. J. Struct. Eng. 136 (11), 1330–1341.
Beck, J.L., Porter, K.A., Shaikhutdinov, R.V., 2003. Simplified estimation of seismic life-cycle costs. Life-cycle performance of deteriorating structures. Life-Cycle Perform. Deterior. Struct. Assess. Des. Manag., 229–236.
Celarec, D., Dolšek, M., 2013. The impact of modelling uncertainties on the seismic performance assessment of reinforced concrete frame buildings. Eng. Struct. 52, 340–354.
Celarec, D., Riccib, P., Dolšek, M., 2012. The sensitivity of seismic response parameters to the uncertain modelling variables of masonry-infilled reinforced concrete frames. Eng. Struct. 35, 165–177.
Choun, Y.S., Elnashai, A.S., 2010. A simplified framework for probabilistic earthquake loss estimation. Probab. Eng. Mech. 25 (10), 355–364.
Cornell, C.A., Jalayer, F., Hamburger, R.O., Foutch, D.A., 2002. Probabilistic basis for the 2000 SAC Federal Emergency Management Agency steel moment frame guidelines. J. Struct. Eng. 128 (4), 526–533.
Coyle, H.M., Reece, L.C., 1966. Load transfer for axially loaded piles in clay. J. Soil Mech. Found. Div., 1–26.

Dasse Design Corporation, (2007). Cost Advantages of Buckling Restrained Braced Frame Buildings. Report 06B260. ⟨http://www.starseismic.net/wp-content/uploads/2013/08/Dasse_Cost_Study.pdf⟩.
Dolsek, M., 2009. Incremental dynamic analysis with consideration of modeling uncertainties. Earthq. Eng. Struct. Dyn. 38, 805–825.
Dolsek, M., 2012. Simplified method for seismic risk assessment of buildings with consideration of aleatory and epistemic uncertainty. Struct. Infrastruct. Eng. 8 (10), 939–953.
Donovan N.C. A statistical evaluation of strong motion data including the February 9, (1971). San Fernando Earthquake. In: Proceedings, 5th world conference on earthquake engineering, Vol. 2. 1973. Paper 155.
Ellingwood, B., Galambos, T.V., MacGregor, J.G., Cornell, C.A., 1980. Development of a Probability-Based Load Criterion for American National Standard A58. National Bureau of Standards, Washington, DC, p. 222.
Ellingwood, B.R., Wen, Y.K., 2005. Risk-benefit-based design decisions for low probability/ high consequence earthquake events in Mid-America. Prog. Struct. Eng. Mater. 7, 56–70.
FEMA, 2000. Recommended seismic design criteria for new steel moment frame buildings. SAC Joint Venture, Federal Emergency Management Agency, Washington, DC.
FEMA-227, Federal Emergency Management Agency, (1992b). A benefit-cost model for the seismic rehabilitation of buildings, Vols. 1 and 2, 227, 228.
Fragiadakis, M., Lagaros, N.D., Papadrakakis, M., 2006. Performance-based multiobjective optimum design of steel structures considering life-cycle cost. Struct. Multidiscip. Optim. 32, 1–11.
Gang, Li, Dayong, Zhang, Qianjin, Yue, 2009. Life-cycle cost-effective optimum design of ice-resistant offshore platforms. J. Offshore Mech. Arct. Eng. 131, 1–9.
Gencturk, B., 2013. Life-cycle cost assessment of RC and ECC frames using structural optimization. Earthq. Eng. Struct. Dyn. 42, 61–79.
Goda, k, Lee, C.S., Hong, H.P., 2010. Lifecycle cost–benefit analysis of isolated buildings. Struct. Saf. 32, 52–63.
Goda, K., Hong, H.P., 2006. Optimal seismic design considering risk attitude, societal tolerable risk level, and life quality criterion. J. Struct. Eng. 132, 2027–2035.
Hanai, T., Fukuwa, N., Mori, Y., Minagawa, T., 2003. Base-isolated houses with restricted displacement according to seismic grade and its life-cycle-cost. J. Struct. Construct. Eng. 572, 89–96.
Haselton, C.B., 2006. Assessing seismic collapse safety of modern reinforced concrete moment frame buildings. Stanford University.
Hays W.W., (1980). Procedures for estimating earthquake ground motions. US geological survey professional paper 1114. Washington (DC).
HAZUS, 2003. MH MR3 technical manual. Federal Emergency Management Agency. FEMA, Washington (DC).
Ibarra, L.F., 2003. Global collapse of frame structures under seismic excitations. Department of Civil and Environmental Engineering, Stanford University, Stanford, CA.
ISO fixed steel offshore structures code 19902, (2003). Component-based calibration of North West European annex for environmental load factors. Research report 088.
Jeong, S.H., Elnashai, A.S., 2007. Probabilistic fragility analysis parameterized by fundamental response quantities. Eng. Struct. 29 (6), 1238–1251.
Kala, Z., 2005. Sensitivity analysis of the stability problems of thin-walled structures. J. Construct. Steel Res. 61, 415–422.
Kennedy, R., Short, S., Merz, K., Tokarz, F., Idriss, I., Powers, M., Sadigh, K., 1984. Engineering Characterization of Ground Motion-Task I: Effects of Characteristics of Free-Field Motion on Structural Response. U.S. Regulatory Commission, Washington, D.C..
Kim, J., Park, J.H., Lee, T.H., 2011. Sensitivity analysis of steel buildings subjected to column loss. Engineering Structures 33, 421–432.
Kwon, O.S., Elnashai, A.S., 2006. The effect of material and ground motion uncertainty on the seismic vulnerability curves of RC structures. Eng. Struct. 28 (2), 289–303.
Kwon, O.S., Elnashai, A.S., 2010. Fragility analysis of a highway over-crossing bridge with consideration of soil-structure interaction. Struct. Infrastruct. Eng. 6, 159–178.
Lagaros, N.D., 2007. Life-cycle cost analysis of design practices for RC framed structures. Bull. Earthq. Eng. 2007 (5), 425–442.
Lagaros, N.D., Fotis, A.D., Krikos, S.A., 2006. Assessment of seismic design procedures based on the total cost. Earthq. Eng. Struct. Dyn. 2006 (35), 1381–1401.
Lagaros, N. D., Charmpis, D. C., Papadrakakis, M., (2005). Assessing the seismic vulnerability of elasto- lastic structures with stochastic properties. In: Proceedings of the 6th European Conference on Structural Dynamics (EURODYN 2005), Paris, France, September 4–7, 2005.
Lamprou, A., Jia, G., Taflanidis, A.A., 2013. Life-cycle seismic loss estimation and global sensitivity analysis based on stochastic ground motion modeling. Eng. Struct. 54, 192–206.
Lee, T.H., Mosalam, K.M., 2005. Seismic demand sensitivity of reinforced concrete shear-wall building using FOSM method. Earthq. Eng. Struct. Dyn., 1719–1736.
Liu, M., Wen, Y.K., Burns, S.A., 2004. Life cycle cost oriented seismic design optimization of steel moment frame structures with risk-taking preference. Eng. Struct. 26 (10), 1407–1421.
Liu, M., Burns, S.A., Wen, Y.K., 2005. Multi-objective optimization for performance-based seismic design of steel moment frame structures. Earthq. Eng. Struct. Dyn. 34 (3), 289–306.
Luco, N., Cornell, C.A., 2000. Effects of connection fractures on SMRF seismic drift demands. J. Struct. Eng. 126 (1), 127–136.
Luco, N., and Cornell, C. A., 1998. Effects of random connection fractures on the demands and reliability for a 3-story pre-Northridge SMRF structure. In: Proc. of the 6th U.S. National Conf. on Earthquake Engineering, Earthquake Engineering Research Institute, Oakland, Calif.
Martinez-Rueda, J., 1998. Scaling procedure for natural accelerograms based on a system of spectrum intensity scales. Earthq. Spectra 14, 135–152.
Mathoworks, Matlab R2011a, ⟨http://www.mathworks/products/matlab⟩.
Matlock, H., 1970. Correlations for design of laterally loaded piles in soft clay. In: Proceedings of Offshore Technology Conference, Richardson, Houston, TX, USA (pp. 577–594).
Newmark N.M., Hall W.J., Mohraz B., 1973. A study of vertical and horizontal earthquake spectra. USAEC report WASH-1255. Washington (DC).
Nour El-Din, M., Kim, J., 2014. Sensitivity analysis of pile-founded fixed steel jacket platforms subjected to seismic loads. Ocean Eng. 85, 1–11.
Nour El-Din, M., Kim, J., 2015. Seismic performance of pile-founded fixed jacket platforms with chevron braces. Struct. Infrastruct. Eng. 11 (6), 776–795.
Pacific Earthquake Engineering Research (PEER) Center, 2013. Strong motion database, Berkeley, Calif., U.S.A. (accessed 08.08.13.).
Padgett, J.E., DesRoches, R., 2007. Sensitivity of seismic response and fragility to parameter uncertainty. J. Struct. Eng. ASCE, 1710–1718.
Pinto, P.E., Giannini, R., Franchin, P., 2004. Seismic Reliability Analysis of Structures. IUSS Press.
Porter, K.A., Beck, J.L., Shaikhutdinov, R.V., 2002. Sensitivity of building loss estimates to major uncertain variables. Earthq. Spectra 18 (4), 719–743.
PTTEP International, 2010. Provision of earthquake specific engineering services (site study) for Myanmar Engineering Zawtika Project, Geotechnical Earthquake Engineering Addendum, Doc. No. 09-214-H4.
RS Means Corp., 1997. Means assemblies cost data. Kingston (MA).
SAP2000, 2005. Structural Analysis Program, Version 10 Analysis Reference Manual. Computers and Structures, Inc., Berkeley, California, USA.
Shome, N., Cornell, C., Bazzurro, P., Carballo, J., 1998. Earthquakes, records, and nonlinear responses. Earthq. Spectra 14, 469–500.
Smith, A.K.C., Turner, R.C., Mackenzie, B., 1998. The implications of the load and resistance factor design method for North Sea pile design. Offshore Site Investigation and Foundation Behavior 'New Frontiers' International Conference, London.
Takahashi, Y., Der Kiureghian, A., Ang, A.H.S., 2005. Life-cycle cost analysis based on a renewal model of earthquake occurrences. Earthq. Eng. Struct. Dyn. 33, 859–880.
Vorechovsky, M., Novak, D., 2003. Statistical correlation in stratified sampling. In: Der Kiureghian, A., Madant, S., Pestana, J.M. (Eds.), ICAPS 9 Proceedings of International Conference on Applications of Statistics and Probability in Civil Engineering. Millpress, Rotterdam, San Francisco, pp. 119–124.
Wen, Y.K., Kang, Y.J., 2001a. Minimum building life-cycle cost design criteria I: methodology. J. Struct. Eng. (ASCE) 127 (3), 330–337.
Wen, Y.K., Kang, Y.J., 2001b. building life-cycle cost design criteria II: applications. J. Struct. Eng. (ASCE) 200 (3), 338–346.
Wen, Y.K., Ellingwood, B.R., Bracci, J., 2004. Vulnerability Function Framework for Consequence-Based Engineering. Mid-America Earthquake Center, University of Illinois at Urbana-Champaign.
Yun, S.Y., Foutch, D.A., 2000. Performance Prediction and Evaluation of Low Ductility Steel Moment Frames for Seismic Loads. SAC Joint Venture, Richmond, Calif.
Zona, A., Ragni, L., Dall'Asta, A., 2012. Sensitivity-based study of the influence of brace over-strength distributions on the seismic response of steel frames with BRBs. Eng. Struct. 37, 179–192.
Zou, X.K., Chan, C.M., Li, G., Wang, Q., 2007. Multi-objective optimization for performance-based design of reinforced concrete frames. J. Struct. Eng. 133 (10), 1462–1474.